

New development of atomic layer deposition: processes, methods and applications

Peter Ozaveshe Oviroh^a, Rokhsareh Akbarzadeh^a, Dongqing Pan^b, Rigardt Alfred Maarten Coetzee^a and Tien-Chien Jen^a

^aMechanical Engineering Science Department, Faculty of Engineering and the Built Environment, University of Johannesburg, Johannesburg, South Africa;

^bDepartment of Engineering Technology, University of North Alabama, Florence, AL, USA

ABSTRACT

Atomic layer deposition (ALD) is an ultra-thin film deposition technique that has found many applications owing to its distinct abilities. They include uniform deposition of conformal films with controllable thickness, even on complex three-dimensional surfaces, and can improve the efficiency of electronic devices. This technology has attracted significant interest both for fundamental understanding how the new functional materials can be synthesized by ALD and for numerous practical applications, particularly in advanced nanopatterning for microelectronics, energy storage systems, desalinations, catalysis and medical fields. This review introduces the progress made in ALD, both for computational and experimental methodologies, and provides an outlook of this emerging technology in comparison with other film deposition methods. It discusses experimental approaches and factors that affect the deposition and presents simulation methods, such as molecular dynamics and computational fluid dynamics, which help determine and predict effective ways to optimize ALD processes, hence enabling the reduction in cost, energy waste and adverse environmental impacts. Specific examples are chosen to illustrate the progress in ALD processes and applications that showed a considerable impact on other technologies.

ARTICLE HISTORY

Received 9 January 2019

Revised 21 March 2019

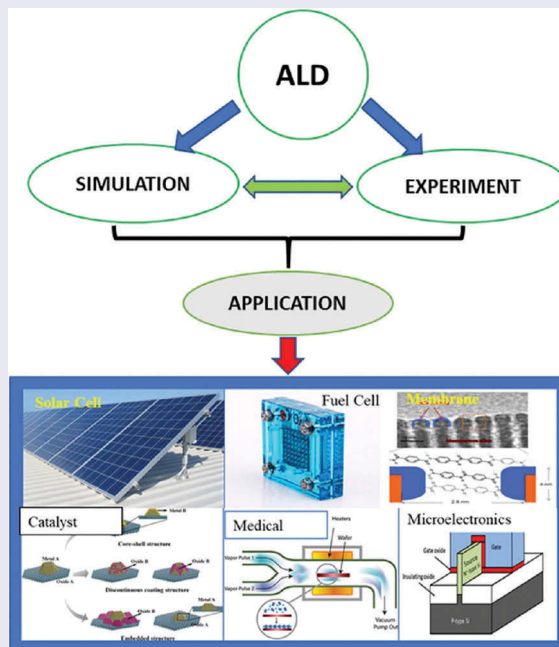
Accepted 22 March 2019

KEY WORDS

Atomic layer deposition;
Thin film; Molecular
dynamics; Computational
fluid dynamics

CLASSIFICATION

10 Engineering and
Structural materials; 102
Porous / Nanoporous /
Nanostructured materials;
306 Thin film / Coatings; 400
Modeling / Simulations



1. Introduction

1.1. Definition of ALD

Atomic layer deposition (ALD) is a thin film deposition technique where chemical precursors are sequentially

introduced to the surface of a substrate where they chemically react directly with the surface to form sub-monolayers of film. As the name implies, it is fundamentally atomic in nature and results in the precise deposition of films on the surface of a selected substrate at the atomic scale.

CONTACT Peter Ozaveshe Oviroh  ovir2009@gmail.com; Tien-Chien Jen  tjen@uj.ac.za  Mechanical Engineering Science Department, Faculty of Engineering and the Built Environment, University of Johannesburg, Johannesburg 2006, South Africa

© 2019 The Author(s). Published by National Institute for Materials Science in partnership with Taylor & Francis Group.

This is an Open Access article distributed under the terms of the Creative Commons Attribution License (<http://creativecommons.org/licenses/by/4.0/>), which permits unrestricted use, distribution, and reproduction in any medium, provided the original work is properly cited.

1.2. Background

The concept of ALD was first introduced by Prof. V. B. Aleskovskii in his PhD work in 1952 [1]. The work was consolidated in another work on the process together with Prof. Kolt'sov in 1960, with which they published the principles of ALD with the title of 'Molecular Layering' [1].

In 1970, Dr. Tuomo Suntola along with other researchers developed an industrial thin film deposition technology and called it 'atomic layer epitaxy' (ALE) [2]. This technology found its first application in thin-film electroluminescent (TFEL) flat panel display [2], and the technology and materials selection has grown over years and find applications in photovoltaics, catalysis, semiconductor devices and many others [3].

ALD occurs by chemical reactions of two or more precursors injected alternately into a chamber where a substrate is placed at a given temperature and pressure to enable materials deposition on the substrate's surface layer by layer [4]. Unlike chemical vapour deposition (CVD) and other similar deposition methods, in ALD the precursors are not pumped simultaneously, they are pulsed sequentially. Although there are similarities between ALD and CVD, the distinction lies in the self-limiting characteristics for precursor adsorption, alternate and sequential introduction of the precursors and reactants [5].

In addition, ALD as a thin film deposition method is becoming attractive because of its unique uniform deposition and conformal films on complex three-dimensional surfaces [6,7]. Thin film deposition can be divided into three main categories: the liquid, gas and solid based deposition methods which include but are not limited to physical vapour deposition

(PVD) and the chemical vapour deposition (CVD). ALD can be counted as the most advanced version of the traditional CVD process [8]. In the ALD process, alternative pulses of precursor vapour and purge gas are introduced into the reactor, resulting in thin film growth due to self-saturating reactions with accessible surface groups, leading to a self-limited growth of a (sub) monolayer of material [9]. The process of ZnO thin film deposition by an ALD process is illustrated in Figure 1. As it is seen in Figure 1, the ALD process for two precursors are usually used in depositing metal oxide films; one is the metal source and the other is the oxygen source (oxidant) [10].

The synthesis of aluminium oxide (Al_2O_3) thin film is another example of an ALD process where trimethyl aluminium (TMA) and water in the thermal ALD reactor have been used to create a thin film [11–13]. The steps of a single cycle deposition process are as follows:

- (1) Exposure of the first precursor in the reactor chamber to form a layer on the substrate
- (2) Purge the excess first precursor and the by-products
- (3) Exposure of the second precursor
- (4) Purge or evacuation of the excess second precursor and by-products
- (5) The process is repeated until the required film thickness is achieved.

The above processes are demonstrated in Figure 2.

This review looks at the progress in ALD in light of the process and product development in both areas of computational and experimental methodologies in

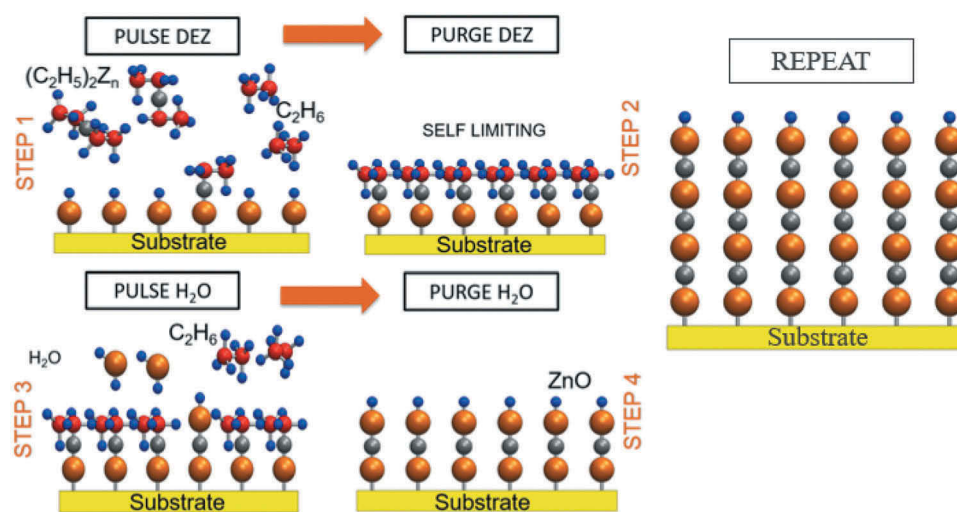


Figure 1. Illustration of ALD for ZnO thin film deposition. Adapted with permission from [11].

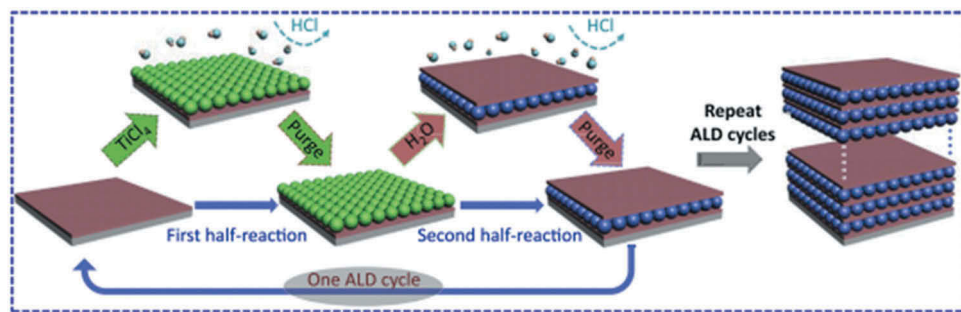


Figure 2. A model ALD process for depositing TiO_2 on hydroxyl groups functionalized substrate using TiCl_4 and H_2O as precursors. Adapted with permission from [13], copyright Elsevier 2017.

this field to date. This will also provide insights into the outlook of this emerging technology.

1.3. Thin film applications

Thin film can be defined as a layer of material that its thickness ranges from nanometre to several micrometres. Thin film can be produced using varieties of techniques which are based on either physical or chemical processes. The thin film coating finds applications in many fields such as semiconductors [5,14–18], which enables the design of smaller semiconductor for a smaller device while performing better with higher energy efficiency. Application of thin film in fabricating batteries has also been reported to improve the efficiency of the batteries [13,19–28]. The solar industry is another industry which vastly relies on thin film technology as thin film is a potential alternative to present solar panels since it poses advantages such as easy production and higher flexibility [20,27,29–35]. Thin film finds another application in water purification and it can reduce the size of purification unit and also increases the efficiency such as in membrane technology and also fabrication of photocatalyst thin film for water treatment [36–43]. Thin film is very useful in wastewater treatment where the application of nanomaterial as a photocatalyst for pollution abatement is needed [44–47]. Applications of a thin film instead of nanopowder have been reported to be an effective method which immobilizes the nanomaterial on a surface of substrates and avoid the cumbersome separation of nanosize materials form water and wastewater. Air purification is another area where nanomaterial can be used as thin film [48,49]. Automobile industries can be accounted as another big applicant of thin film as it finds application in nearly every part of it, for example, applying thin film can reduce the size and improve the life of different parts [50]. Thin film has a huge application on medicine and medical devices, for instance, it can reduce the size of medical devices and make their application easier, more durable and secure [40,51–53].

1.4. Comparison of ALD with other coating techniques

There are several studies that have compared ALD with other film deposition techniques. Here we have summarized these comparisons in tabulated forms. Table 1 presents different types of film deposition methods, their advantages and applications of each technique.

In the industry, the PVD and CVD have been the popular deposition methods, however, ALD has been recognized as the leading emerging technology as nanometre-size layer thickness or pinhole free layers are becoming more important [54].

In comparison to CVD which relies on high temperatures to decompose the precursor at the substrate surface, ALD processes are performed at lower temperatures. The growth rate of ALD is related to the precursor's flux at the substrate. It is complicated to determine the growth rate and it often operates within the temperature window, the point where the temperature and concentration of the precursor per pulse, and the purge times are balanced and the growth per cycle (GPC) is stable [54].

Table 2 provides the general overview and physical properties of the thin film deposited by the ALD process in comparison to other thin-film fabrication techniques which are similar to ALD. In this study, the authors have compared different deposition techniques based on the design parameters. As presented in Table 2, ALD has noteworthy advantages such as uniformity and control of deposition. However, due to its inherent layer by layer deposition, the deposition rate in the ALD process is low, which is the major drawback of this process.

1.5. Advantages and disadvantages of ALD

The outstanding feature of ALD in comparison to other deposition techniques such as CVD and PVD is the self-limiting chemisorption of precursors in each half-cycle. This makes ALD unique in sub-nanometre film thickness and conformality control, offering next to (nearly) equal

Table 1. Different types of film deposition methods (adapted from [54]), the sputtering was adapted from [55] while the breath figure method was adapted from [56], with permission.

Method	Description and types	Advantages	Applications
<i>Electroplating</i>	Film formation from chemicals in electrolytic solution placed onto substrate surface with a seed layer on top	Corrosion resistance, decoration, mechanical characteristics improvement, protection barriers, electrical conduction and heat resistance	Metal plating, corrosion resistance, decoration, mechanical characteristics improvement, friction reduction, protection barriers, improved electrical conductivity, heat resistance and radiation protection etc.
<i>Spin coating</i>	Film formation from chemical reaction between liquid-phase sources (often sol-gel) applied onto surface of substrate while spinning	Simplicity and ease of set up, low cost and fast operating system	Photoresists, insulators, organic semiconductors, synthetic metals, nanomaterials, metal and metal oxide precursors, transparent conductive oxides, optical mirrors, magnetic disk for data storage, solar cells etc.
<i>Sputtering</i>	A process of deposition of materials because of bombardment of targets by high energy particles ejected from a source	Deposit a wide variety of metal and metal oxide nanoparticles (NPs) and nanoclusters (NCs), insulators, alloys and composites, and even organic compounds	Silicon wafer, solar panel or optical device, catalysis
<i>Breath figure</i>	A self-assembly process that results in a honeycomb-structured films with micro-pores arranged in honeycomb shape usually formed by water microdroplets condensed on a cool surface from warm, humid air like breath	It is simple and applicable to a wide variety of materials with highly organized honeycomb-like porous surface	Optics, photonics, surface science, biotechnology, and regenerative medicine
<i>Thermal oxidation</i>	Film formation by thermal oxidation of the substrate	Slow oxidation rate, good control of the oxide thickness and high values of breakdown field	Semiconductor industry, transistors, photoresistors, capacitors and field oxides, etc.
<i>Physical vapour deposition (PVD)</i>	Film formation by condensation of gasified source material, directly transported from source to substrate through the gas phase: Evaporation (thermal, E-beam), Molecular beam epitaxy (MBE), Pulsed laser deposition (PLD), Reactive PVD, Sputtering (DC, DC magnetron, RF)	Atomic level control of chemical composition, film thickness, and transition sharpness	Fuel cells, batteries, microelectronics, optical and conducting surfaces, etc.
<i>Chemical vapour deposition (CVD)</i>	Film formation by chemical reaction between mixed gaseous source materials on a substrate surface using: Atmospheric-pressure CVD (APCVD), Low-pressure CVD (LPCVD), Plasma-enhanced CVD (PECVD), Metal-organic CVD (MOCVD)	High growth rates, good reproducibility, epitaxial films growth, good film quality, conformal step coverage	Microelectronics, solar cells, fuel cells, batteries, etc.
<i>Atomic layer deposition (ALD)</i>	A sub-class of CVD with film formation via sequential cycling of self-limiting chemical half-reactions on the substrate surface. Each reaction cycle accounts for the deposition of a (sub) monolayer. The reaction can be activated by thermal energy or plasma enhancement. They can be categorized as: Thermal ALD, Plasma-enhanced ALD (PEALD), Spatial ALD (S-ALD)	High quality films, conformality, uniformity, step coverage	Fuel cells, desalination, microelectronics, capacitors, oxides, catalysts, etc.

Table 2. Comparison of thin film deposition techniques which are similar to ALD (Adapted with permission from Elsevier 2017 [57]).

Property	Deposition Technique					
	CVD	MBE	ALD	PLD	Evaporate	Sputtering
Deposition Rate	Good	Fair	Poor	Good	Good	Good
Film density	Good	Good	Good	Good	Fair	Good
Lack of pinholes	Good	Good	Good	Fair	Fair	Fair
Thickness uniformity	Good	Fair	Good	Fair	Fair	Good
Sharp dopant profiles	Fair	Good	Good	Varies	Good	Poor
Step coverage	Varies	Poor	Good	Poor	Poor	Poor
Sharp interfaces	Fair	Good	Good	Varies	Good	Poor
Low substrate temp.	Varies	Good	Good	Good	Good	Good
Smooth interfaces	Varies	Good	Good	Varies	Good	Varies
No plasma damage	Varies	Good	Good	Fair	Good	Poor

Abbreviations: Chemical vapour deposition (CVD), Molecular beam epitaxy (MBE), Atomic layer deposition (ALD), Pulsed layer deposition (PLD)

Table 3. Advantages and disadvantages of ALD.

Advantages	Disadvantages
<ul style="list-style-type: none"> • High-quality films <ul style="list-style-type: none"> a. Control of the film thickness b. Excellent repeatability c. High film density d. Amorphous or crystalline film e. Ultra-thin films • Conformality <ul style="list-style-type: none"> a. Excellent 3D conformality b. Large area thickness uniformity c. Atomically flat and smooth surface coating • Challenging Substrates <ul style="list-style-type: none"> a. Gentle deposition process for sensitive substrates b. Low temperature and stress c. Excellent adhesion d. Coats Teflon • Low-temperature processing • Stoichiometric control • Inherent film quality associated with self-limiting • Self-assembled nature of the ALD mechanism • Multilayer 	<ul style="list-style-type: none"> • The time required for the chemical reactions • The economic viability • Very high material waste rate • Very high energy waste rate • Intensive nature of the ALD process • Nano-particle emissions <p><i>low deposition rate</i></p>

growth-per-cycle values for identical precursors in different equipment [54].

Table 3 presents the main advantages and disadvantages of the ALD process. ALD can create high-quality film with conformality and most importantly it works at low temperatures. ALD is exceptionally effective at coating surfaces that exhibit ultra-high aspect ratio topographies, as well as surfaces requiring multilayer films with good quality interfaces [54]. However, ALD is facing some challenges as mentioned in Table 3. The ALD process is a high precision process and this often leads to **high precursor gas usage and energy**. Approximately 60% precursor dosage is wasted in the ALD process which implies that **most of the energy has been wasted** as well as the concomitant labour. This low material utilization efficiency is shown to be about 50.4% of TMA deposited on wafers as revealed by experiments [55,56]. For instance, in the Al₂O₃ ALD process, ~4.09 MJ energy is consumed for the deposition of a film with 30 nm thickness and this shows the energy-intensive nature of the ALD process and invariable energy wastage [56,57]. In a previous study on nanoparticle emissions, Al₂O₃ ALD process shows that the total nanoparticle emissions with the diameter of less than 100 nm are in the range of 6.0×10^5 and 2.5×10^6 particles in 25 cycles of Al₂O₃ ALD process [58]. Another drawback in ALD for commercial use is the **cost-effectiveness which is principally due to its deposition rate**; however, this challenge has been partially overcome using spatial atmospheric ALD [58].

1.6. Complex 3D nanostructures

Owing to its conformal and self-limiting surface deposition, ALD has shown premier advantages to fabricate 3D complex nanostructures. A variety of materials such as semiconductors, magnetic materials, noble metals, and insulators are being fabricated using ALD to form 3D

complex nanostructures, which are promising in the applications of high-performance transistors, nanostructures, energy storages and conversion.

Usually, ALD is used to fabricate complex 3D nano-structures [59]. For instance, surface modification of nanoporous materials is being realized through ALD coating with excellent step coverage inside of the porous structures. Such kind of structures with large surface areas with ALD-coated wide-bandgap semiconducting oxides, transparent conducting oxides, and ion conducting oxides have been used for solar cells, lithium-ion batteries, and solid oxide fuel cells [59]. The following table (Table 4) summarized the materials, reactants and templates used in ALD coating of nano-porous structures.

Using diatoms as templates, Lasic et al. [60] demonstrated coating of ultrathin films of titanium oxide (TiO₂) by using titanium chloride (TiCl₄) and water to modify the pore size. Such structures show huge potential in membrane applications in microfluidic systems.

In their work, Zhang et al. [61] used ALD to coat a layer of Al₂O₃ on top of Li depositions on a 3D carbon nanotube sponge (CNTS) structure to protects the Li metal electrode/electrolyte interface in Li-ion-based batteries as illustrated in Figure 3. The ALD-deposited Al₂O₃ layer provided desirable chemical stability and high mechanical strength for Li@ALD-CNTS electrode.

Kim et al. [62] reported a method of using ALD to synthesize crystalline 3D mesoporous ZnO networks based on a self-assembled block copolymer template. Two 3D mesoporous morphologies including a periodic gyroid structure and a random worm-like morphology were fabricated as shown in Figure 4. Metrological examinations showed that the ALD deposited films were uniform in terms of pore size and material composition. Such complex 3D structures are

Table 4. Materials, reactants and templates used in ALD coating of nano-porous structures. Republished with permission from [59].

Materials	Reactants	Temperature	Template
TiO ₂	Ti[OCH(CH ₃) ₂] ₄ /H ₂ O	140 °C	Polycarbonate
ZrO ₂	Zr[OCH(CH ₃) ₃] ₄		
TiO ₂	TiCl ₄ /H ₂ O	105 °C	AAO
ZnO	Zn(C ₂ H ₅) ₂ /H ₂ O	200 °C	AAO
ITO	InCp/O ₃ Tetrakis(dimethylamino)tin/H ₂ O ₂	275 °C	AAO
Ru	Ru(EtCp) ₂ /O ₂	300 °C	AAO
SiO ₂	H ₂ N(CH ₂) ₃ Si(OCH ₂ CH ₃) ₃ /H ₂ O/O ₃	150 °C	AAO
Fe ₂ O ₃	Fe ₂ (OBu) ₆ /H ₂ O	130 °C – 170 °C	AAO
Fe ₂ O ₃	Fe(Cp) ₂ /O ₃	230 °C	AAO
Fe ₂ O ₃ + Fe ₃ O ₄	Fe(Cp) ₂ /O ₂	350 °C – 500 °C	AAO
ZnS	Zn(C ₂ H ₅) ₂ /H ₂ S	120 °C	AAO
Sb ₂ O ₅	(Sb(NMe ₂) ₃) ₂ O ₃	120 °C	AAO
Sb ₂ S ₃	(Sb(NMe ₂) ₃) ₂ H ₂ S	120 °C	AAO
Nb ₂ O ₅	NbI ₃ /O ₃	320 °C	AAO

ITO stands for Indium tin oxide, AAO stands for anodic aluminium oxide, Ru(EtCp)₂ stands for bis(ethytcyclopentadienyl)ruthenium, Sb(NMe₂)₃ stands for Tris(dimethylamido)antimony(III)

attractive for hybrid photovoltaic applications such as fabricating ZnO solar cells.

More applications of using ALD for self-limiting surface modifications to fabricate 3D nanostructures used in energy storage and conversion were reviewed

and summarized in the review [63]. For instance, using ALD, copper indium sulfide (CuInS₂) was deposited into a porous TiO₂ electrode to improve the responsiveness of solar cell compared to the conventional dye-sensitized cells [63].

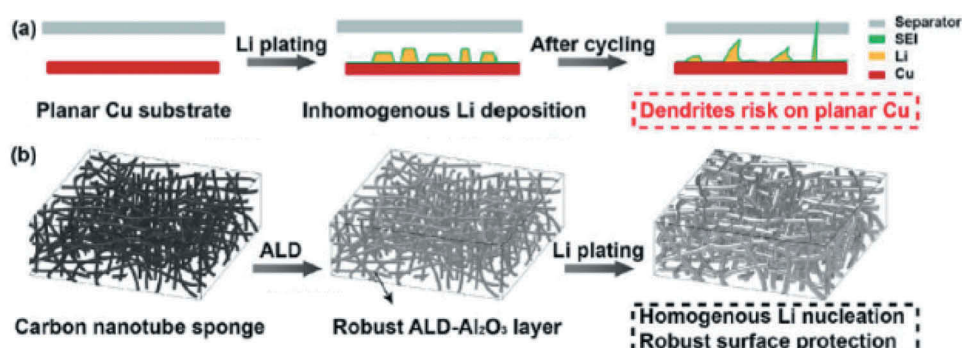


Figure 3. Schematic illustration of the Li deposition process on planar Cu and 3D ALD-CNTS substrates. (a) Inhomogeneous Li deposition resulted in the formation of Li dendrites, which punctured the separator after repeated cycles. (b) A high-specific-surface-area CNTS network with a robust Al₂O₃ layer on the surface ensures homogenous Li nucleation during the Li plating process and forms a stable, dendrite-free Li metal anode.

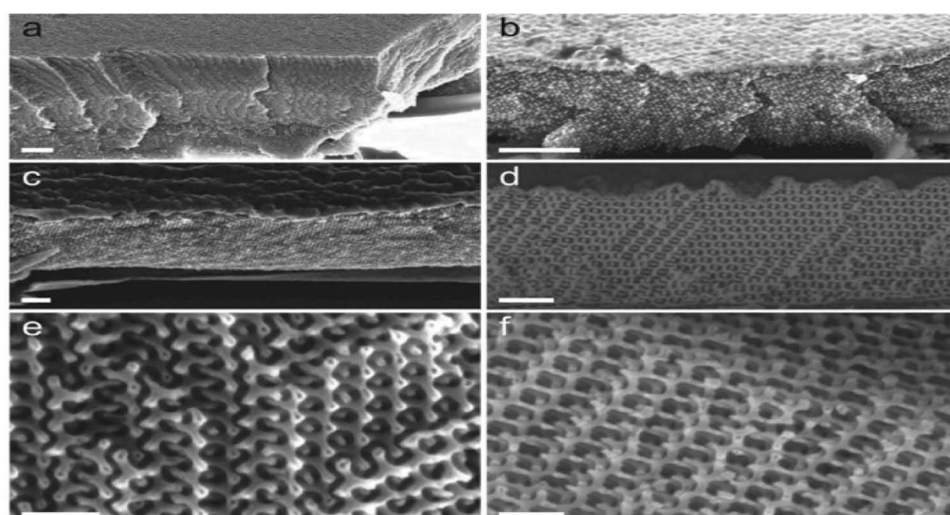


Figure 4. Side-view scanning electron microscopy (SEM) images at a 45° angle of gyroid replication into ZnO: (a) gyroid polystyrene template, (b) as-deposited ZnO-PS hybrid, and (c) ZnO gyroid after annealing at 550 °C. (d,e,f) Different faces of the ZnO gyroid shown in (c). The scale bars correspond to 1 μm for (a) and (b), 400 nm for (c) and (d), 200 nm for (e) and (f).

However, due to the complex structures of the templates, such as porous structures, reactant molecules tend to be confined inside of such complex structures. The precursor flow will be hindered, and hence the reactions can be different from those reactions on a planar surface, in terms of both mechanism of nucleation and growth of the film [63]. To achieve desirable conformal surface coatings, the optimization of ALD process on the 3D structures will require a more detailed understanding of their physical, chemical, and electrochemical properties in order to precisely tune the process parameters.

The specific challenges for the characterization of 3D nanoarchitectures were summarized in the reference [63]. In-lab materials science analyses provide a reasonable understanding of the character of a given nanostructures to optimize synthetic and fabrication strategies. Such metrological techniques include simultaneous differential scanning calorimetry and thermogravimetric analysis to guide thermal treatment of the structure, X-Ray diffraction analysis to provide information on the 'bulk' structure of the solid, and physisorptive analyses to provide surface area, pore volume and the distribution of pore sizes [63].

Samples could be further characterized by field emission scanning electron microscopy, transmission electron microscopy, small-angle neutron scattering, X-ray photoelectron spectroscopy and vibrational spectroscopy, Fourier-transform infrared spectroscopy, and solid-state nuclear magnetic resonance [63].

2. ALD processes

There are different ALD process modes but the most widely used ALD modes are thermal ALD and plasma-enhanced ALD (PEALD). In addition, plasma-assisted or radical-enhanced ALD are also referred to as PEALD. Thermal ALD is mainly a surface-driven process, which occurs exclusively through surface reactions, thus enabling good thickness control and conformality irrespective of the substrate geometry and reactor design. Thermal ALD processes require relatively high temperatures (typically 150–350 °C); this causes a limitation on their applications which can be addressed by PEALD [64].

Table 5. Advantages and disadvantages of PEALD.

Advantages	Disadvantages
Low deposition temperature	Limited conformality
Higher reactivity (shorter deposition times)	More complicated reactor designs
Higher film purity	More complicated reaction chemistry
Wide range of chemistry possible	Potentially poor conformality
Denser films	Lower throughput
Higher throughput	Damage to films
In situ plasma treatment	Additional growth parameter
Lower impurity	

PEALD, also referred to as plasma-assisted ALD (PA-ALD), has high reactivity of the plasma species which enables the reduction of the deposition temperatures without compromising the film quality. It is appreciated especially when the thin films are deposited on temperature-sensitive materials. PEALD can also lead to improved material properties. Furthermore, the reactivity of the plasma facilitates the use of a wider selection of precursors and enables the deposition of materials that are challenging or inaccessible by the means of thermal ALD [65].

Increasing the surface area and volume of an ALD reactor leads to longer pulse and purge time resulting in lower throughput. This is improved by using spatial ALD (SALD), which eliminates the pulse purge chambers with the spatially resolved head by exposing the substrate to a specific precursor based on location, though the quality of the thin film would have been decreased [58]. SALD technique can achieve deposition rates of around 3600 nm/h [7]. Table 4 gives the advantages and disadvantages of plasma enhanced atomic layer deposition. PEALD allows deposition at relatively low temperatures and film properties are better than the ones in thermal ALD [66]. PEALD also provides highly reactive species or catalysts that enhance the reaction thus enabling the use of lower temperatures, as well as a broader range of substrates and precursors for deposition [67]. Therefore, PEALD is useful for the growth of film on the substrates that are heat sensitive. PEALD can also produce highly pure films than the films produced by thermal ALD [68]. Other advantages of the PEALD are the wider choice of precursors, higher growth rate, and process versatility [69]. Table 5 has summarized the advantages and disadvantages of the PEALD method.

Despite the advantages of the process, PEALD also precipitates undesired side-reactions. To derive the maximum advantages, the ALD process should be within this optimum temperature window, else poor growth rates, slow reaction kinetics or precursor condensation and thermal decomposition could occur [7]. As mentioned earlier, the 'ALD temperature window' is the temperature range where the growth is saturated, and it depends on the specific ALD process.

Although PEALD has limited conformity and reactor designs are more complicated, its low deposition temperature makes it valuable for some applications such as capacitors, DRAM, etc. Figure 5 illustrates three types of plasma sources for PEALD at low pressures. The first configuration (a) is called the 'direct plasma', because the substrate is exposed to high energy ions or the deposition surface is in contact with the active plasma. The second configuration (b) is known as a remote plasma system-the contact between plasma and substrate as well as the mild ion energies distinguish remote plasma ALD from radical-enhanced and then the 'radical enhanced' or 'radical assisted' (Figure 5

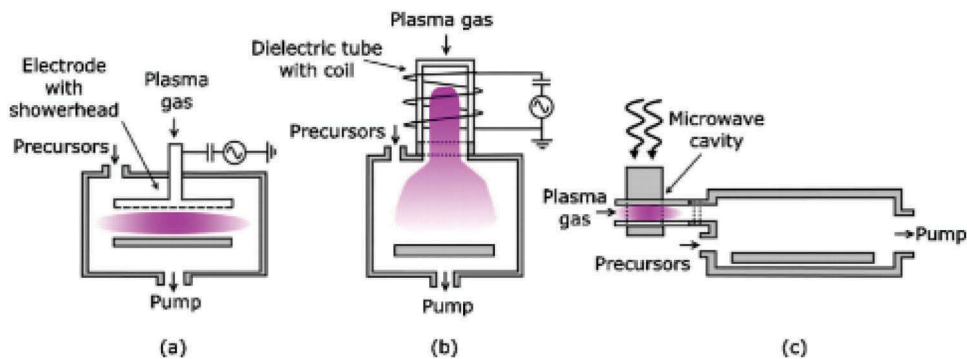


Figure 5. Schematic representation of the three different types of plasma-assisted atomic layer deposition that can be distinguished: (a) direct plasma (b) remote plasma, and (c) radical enhanced. For each type different hardware configurations and plasma sources.

(c)) ALD. Radical enhanced ALD has an advantage that the substrate or growing film are not damaged by energetic plasma species [68] and only the neutral plasma species participate in the deposition process.

Recently a branch of ALD, called the photo-assisted ALD or UV-enhanced ALD, has been developed. There the illumination by UV light is adapted as a part of the ALD cycle. UV exposure has been shown to enhance the surface reactions and lead to improved film properties [65].

3. Methods for studying ALD

Research study on the ALD process is growing into two main categories: numerical and experimental. In the experimental studies, researchers have improved the deposition of the films by adjusting the conditions such as; pressure, temperature, purge time, concentration, etc [4]. The ALD process has quite extensive materials range to choose from however not all materials can be used; hence, the need for simulation to determine and predict which effective reaction pathways are necessary.

Due to its atomic scale deposition which is relative to the feature and reactor scale, the ALD numerical method inherently involves multi-scale analysis. The multi-scale process includes atomic bond formation, species chemisorption/adsorption, chemical kinetics and film deposition. It also includes a reactor-scale that involves material selections/interactions, geometry effects, and fluid and energy transport on a macroscopic level [70–77]. A challenge of the feature and reactor scales is that neither addresses the other limitations placed on the prediction capability of the deposition process over the substrates [78–81].

The mesoscopic scale is introduced as the third scale to assist in this problem. At the mesoscopic scale simulation, the continuum laws are still valid. This scale also obtains its net fluxes from the feature densities. The mesoscopic scale couples-decouples between the scale processes by evaluating an element on the reactor scale grid [78–81]. A more detailed

description of the mesoscopic scale will be illustrated in the next section.

Good exposure of the substrate surface is effective to enhance saturation in the ALD process. High sticking probability can be achieved by modification of the surface or by controlling the chemistry of the reaction. To achieve true ALD growth, the purging time between the precursors' exposure time should be sufficient; if not there might be a CVD mode growth due to gas phase precursors mixing, which will lead to poor conformality due to the gas phase reaction [5]. Time for getting saturation is much longer for heavier molecules. The molecular flux is inversely proportional to the square root of the molecular weight.

Remmers et al. [82] were able to develop a procedure using the Gauss–Jordan factorization to separate the modes of thin film deposition with particular interest on ALD because of the cyclic dynamic behaviour and complexity in defining the reactions process on amorphous films. They represented the growth process in the modelling by formulating the full set of adsorption, desorption, and surface reactions into two reaction mechanism cycles, each of which can produce an independent limit-cycle solution. According to Travis and Adomaitis [52], the deposition rate in ALD largely depends on the instantaneous growth state of the surface and this changes throughout each exposure and purge time.

In comparing modelled results and experimental results of the ALD process, Jones et al. [83] set up a model to predict the chemical species in a reactor as a function of time and space to give an optimal ALD process both the experimental and modelled results had a good agreement. The modelled result confirmed that the increased dissociation rate decreases the overall concentration in the chamber irrespective of the pressure. Scale-up analysis of continuous cross-flow atomic layer deposition reactor designs was reported by Holmqvist et al. [84]. They identified the optimal scaling rules in maximizing the

utilization of precursors in the system for a fixed growth rate and relative uniformity.

3.1 Numerical methods

3.1.1. Knudsen number

In ALD simulation by Knudsen number method, both very large and very small Knudsen numbers (K_n) can coexist [76]. The Knudsen number depends on the gas flows pressure, temperature, and the characteristic reactor dimensions. It defines the ratio of the mean free path and the characteristic length. Likewise, it can also be defined as the molecule-wall to molecule-molecule collisions. The Knudsen number is used to indicate which formulation should be used for a specific situation as the mean free path becomes comparable with, or even larger than, the characteristic length (high K_n number), at which the particle nature of matter must be clearly accounted for, since the continuum assumption breaks down, particularly in the area of micro-scale or nano-scale processes [85]. A flow type can be characterized as a continuum with $K_n < 0.1$, free molecular where $K_n \geq 10$, or transitional in which $10 > K_n > 0.1$ [86,87]. To elaborate, the Navier-Stokes equations with no-slip boundary conditions can be used to simulate very small Knudsen numbers (continuum flows) or utilize statistical mechanics at large Knudsen numbers where the Navier-Stokes equation no longer upholds (molecular flows) [88,89]. At intermediate values of K_n , kinetic models based on the Boltzmann transport equation capture the influence of both transport and collisions

among the molecules; this is called the transition regime.

The Knudsen number can be expressed as:

$$K_n = \frac{\lambda}{d}$$

The mean free path (λ) can be found as

$$\lambda = \frac{k_B T}{p \sqrt{2\pi d_g^2}}$$

where p is the fluid pressure, d_g the effective diameter of the molecule, k_B the Boltzmann constant ($1.3807 \times 10^{-23} \text{ J/K}$), T the temperature of the fluid (K), and d the characteristic length [90].

Along with the Knudsen number, other influential properties arise to limit and define the numerous simulation techniques that are used to quantify the ALD process. These properties include but not limited to computational efficiency, system complexity, and simulation size. In Figure 6, the relation between these properties and simulation methods are illustrated. It can be deduced from this illustration that as the assumption of a volume with no particle space in between moves (continuum approach) to a cluster of small particles (molecular dynamics (MD)). The Knudsen number and system complexity per volume will increase, although the computational efficiency per volume and system size will decrease. These models can range from very fundamental solutions of sets of simple interactions of particles (such as molecular dynamics) to systems in which the individual particles are replaced by continuum fluid

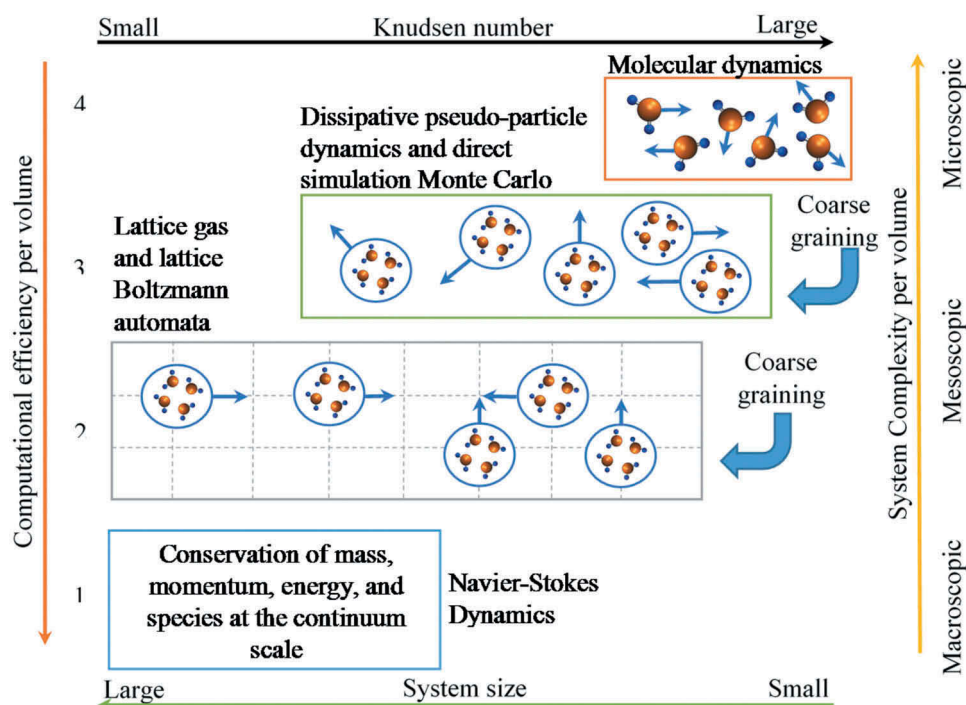


Figure 6. Various methods in describing fluid flow at different levels (modified with permission from Liao and Jen [91] and Coetzee and Jen [11]).

elements estimations (such as the Navier-Stokes equations) [85]. This can be organised from the most fundamental level molecular dynamics (MD), Monte Carlo method, the Lattice Boltzmann Method, to the continuum approach.

3.1.2. Monte Carlo

3D (three-dimensional) Monte Carlo model was used by Cremers et al. [92] to compare the deposition of an infinite array of holes and infinite arrays of pillars using atomic layer deposition on large 3D surface area. They observed that the required exposure to conformally coat an array of holes is determined by the height to width ratio of the individual holes and is independent of their spacing in the array. In studying the conformality of plasma enhanced ALD (PEALD) using the Monte Carlo method, Knoops et al. [93] used the recombination probability, the reaction probability and the diffusion rate of particles to observe the conformal deposition in high aspect ratio structures (step coverage). They identified three deposition positions: a reaction limited regime, a diffusion limited regime and a recombination limited regime. From their findings, conformal deposition can be achieved in high aspect ratio structures with a low value of recombination probability. Shirazi and Elliott [88] studied the atomistic kinetics of atomic layer deposition using the Monte Carlo method derived from density functional theory (DFT) [94]. They looked at the early stage adsorption of the ALD precursor, the surface proton kinetics, the steric effects, influence of remaining fragments on adsorption sites, densification of the precursor, migration, and cooperation of the precursors. They concluded that the essential chemistry of the ALD reactions depends on the local environment at the surface.

3.1.3. Molecular dynamics

Molecular dynamics (MD) is a numerical method that uses Newton's equations of motion for computationally simulating the movements of atoms and molecules. The techniques depend on the description of the interaction of molecules-force field and are extensively used in chemistry, physics, biophysics and biochemistry. MD more often is about developing quantitative predictions of molecular shape, sizes, flexibilities, the interactions with other molecules, its behaviour under pressure, and the relative frequency of one state or conformation compared to the others [95]. Using Newton's equation of motions, the simulation calculates the forces between the atoms at each time step and updates the positions of the atoms at the following time step [96]. High costs and difficult chemical management associated with ALD studies have made more researchers to conduct numerical modelling of the ALD process to understand and study the operation process. In modelling, further insight into the ALD process is gained, hence minimizing the

precursors' inputs and wastes and also reduces the potential environmental impacts in future industrial productions [97].

As compared to other modelling methods, there are few studies using molecular dynamics for ALD modelling. In MD simulations the non-bonded interactions between atoms that are being considered and calculated using the Lennard-Jones potential parameters and the columbic potentials [96,98–100].

$$E = E_{vdW} + E_{Coulombic}$$

Where

$$E = 4\epsilon \left[\left(\frac{\sigma}{r} \right)^{12} - \left(\frac{\sigma}{r} \right)^6 \right] + \frac{q_i q_j}{\epsilon_d r}$$

ϵ and σ are the well depth of potentials between any two atoms and the distance between any two atoms, respectively. The charges between the two atoms i and j are $q_i q_j$, r is the distance between atoms i and j , and ϵ_d is the dielectric constant.

Computational software like reactive force-field (ReaxFF) [101] and DFT [102–104] can be used to gain further insight into the dynamics of the atomic layer deposition process [101]. ReaxFF interatomic potential is a powerful computational tool for exploring, developing and optimizing material properties [101]. ReaxFF is a force-field technique that uses the bond order concept in modelling the interactions in a chemical system [105]. While DFT is a computational method that derives properties of the molecule based on a determination of the electron density of the molecule. It calculates the molecular energy from the electron density, deliver a force field of high accuracy and relatively computational simplicity and efficiency.

Other software, such as LAMMPS [38,106–109], NAMD [53], GROMACS, CHARMM [53] and AMBER [95,100] is also used for molecular dynamics simulation. For instance, by using LAMMPS for molecular dynamics simulation, Hieranian et al. [109] demonstrated that a single layer of molybdenum disulfide (MoS_2) can effectively separate ions from water. They investigated the desalination of water through (MoS_2) as a function of chemistry, pore size, hydrostatic pressure and geometry. To have efficient desalination, the sizes of pores should be such that both the water filtration and ion rejection are optimized. In one hand large pores do not effectively reject ions while very small pores permeation rate is low. Atomic layer deposition is effective in addressing such situations. Hu et al. [110] used MD to study and predict the influence of the initial surface composition and process temperature on the roughness of the surface, the growth rate and growth mode of the film deposition. Timo and Kari [111] in the study of the atomic

layer deposition of alumina by TMA–H₂O-process, they used MD simulation to study the water reaction mechanism with alumina to obtain more insight on the surface mechanisms and energetics which according to them is essential in the design and optimization of the ALD process.

There are studies that provide more insight into molecular dynamics and have explained from basic to advance [99,112,113].

There are other softwares that have been developed with a graphical user interface (GUI) like QuantumATK [104,114] and Lammpsfe that can also be used for ALD molecular dynamics study.

3.1.4. Computational fluid dynamics (CFD)

The computational fluid dynamics method (CFD) involves a continuum approach that has the smallest Knudsen number ($Kn < 0.1$). Intrinsically, this ends with a numerical method that has the highest computational efficiency per volume. Due to this technique treating the fluid as a continuous medium, it illustrates a fully filled domain with no space between the molecule particles. The CFD method attempts to solve the ALD process numerically by applying the governing equations of conservation of mass, momentum, energy, and species transport [12,89,115–118]. These processes are presented by corresponding partial differential equations (PDEs) that are solved numerically on defined nodes in a mesh domain. However, in literature due to the complexity of this fabrication process, studies favoured and focused purely on the mechanical [87,119–122] or the chemistry aspects [52,123] separately. Although this is said, in the past few years researchers [4,13,77,89,116,117,124,125] have applied this technique to combine both mechanical and chemical aspects, in which the necessary chemical data is obtained through the Density Function Theory (DFT) chemical simulation techniques or by chemical reaction experimentation [126]. The DFT technique plays a crucial role in the CFD modelling method. The DFT technique incorporates the required data to simulate the heterogeneous and homogenous reactions within the ALD process, including distinguishing different chemical recipe adsorption/desorption kinetics properties [73,127]. The analysis by combined DFT/CFD is currently rare, however, gaining importance as ALD is moving forward into the industrial realm.

Finally, these properties are utilized within the governing equations by coupling and decoupling the chemical reactions source terms from the prior governing equations. These modelling steps governing equations are expressed as:

$$\frac{\partial \rho}{\partial t} + \nabla \cdot (\rho \vec{v}) = 0$$

$$\frac{\partial \rho \vec{v}}{\partial t} + \nabla \cdot (\rho \vec{v} \vec{v}) = -\nabla P + \nabla \tau + \rho \vec{g} + \vec{F}$$

$$\frac{\partial \rho E}{\partial t} + \nabla \cdot (\vec{v}(\rho E + \rho)) = \nabla \cdot \left(k_{eff} \nabla T - \sum_i^{h_i} J_i \right) + R_r$$

$$\frac{\partial(\rho Y_i)}{\partial t} + \nabla \cdot (\rho \vec{v} Y_i) = -\nabla \cdot \vec{J}_i + R_i$$

where J , k_{eff} and R resemble the diffusion flux term, effective conductivity, and reaction source term, respectively.

The r^{th} irreversible surface reaction can be shown as the following general form:

$$\begin{aligned} & \sum_{i=1}^{N_g} g'_{i,r} G_i + \sum_{i=1}^{N_b} b'_{i,r} B_i + \sum_{i=1}^{N_s} s'_{i,r} S_i \\ &= \sum_{i=1}^{N_g} g''_{i,r} G_i + \sum_{i=1}^{N_b} b''_{i,r} B_i + \sum_{i=1}^{N_s} s''_{i,r} S_i \end{aligned}$$

where G , B and S correspond to the gaseous species, the bulk species, and the site species, respectively. The molar reaction rate for the irreversible surface reaction can be calculated as follows:

$$\begin{aligned} R_r = & k_{f,r} \left(\prod_{i=1}^{N_g} [C_i]_{wall}^{\eta'_{i,gr}} \right) \left(\prod_{i=1}^{N_s} [S_j]_{wall}^{\eta'_{i,sr}} \right) \\ & - k_{b,r} \left(\prod_{i=1}^{N_g} [C_i]_{wall}^{\eta''_{i,gr}} \right) \left(\prod_{i=1}^{N_s} [S_j]_{wall}^{\eta''_{i,sr}} \right) \end{aligned}$$

These equations can be utilized to derive properties of interest in the ALD process focusing on macroscopic parameters, such as the mass deposition rate (\dot{m}_{dep}) that can be obtained at the substrate surface as:

$$\dot{m}_{dep} = \sum_{i=1}^{N_b} M_{w,i} \hat{R}_{i,bulk}$$

Shaeri [89] utilised CFD technique to investigate the reactor inlet position, multi inlets and the effects of high substrate temperatures [10,89]. These studies were comparable to experimental results and illustrated the effects of the mass fraction, coverage, deposition rate and growth rate. Pan et al. [115] also focussed on examining the geometrical effect of gap size on a spatial ALD. They also investigated with experimental validation where the effect of concentration and pumping pressures, pulse/purge times, gap sizes, heating temperatures and flow rates were studied [4,115]. Deng et al. [128] attempted to optimise the ALD process by quantitatively analysing the temperature, precursor mass fractions, mass flow and pressure. They concluded that while higher temperature increased the growth rate and accelerated the surface deposition processes, it had little influence on precursor distribution in the reactor chamber. Intrinsically, their simulation and experimentation also revealed that gas velocity decided the mass flow rate and chamber pressure as the determinant factor for minimising the cycle time.

Holmqvist et al. [121] investigated the controlling parameters on the deposition of the ZnO thin film in a continuous cross-flow ALD reactor. The study oriented towards the optimisation and control of the film thickness profile by evaluating the impact of changing operating parameters such as the local coordinate variable, process cycles, and temperature. In a second study, Holmqvist et al. [120] showed that the model predictions of the spatially dependent film thickness profile were in good agreement with both calibration and validation experimental data, respectively, under a wide range of operating conditions.

To further understand the ALD process, the reactor geometrical design also plays a crucial role. These studies may reveal optimal parameter conditions, defect in the ALD recipe, chemical distribution and dosage requirements, thermal flow effect, among others. The studies by Shaeri [89] and Pan et al. [115] that were previously mentioned have been accomplished by means of utilising a typical Cambridge Nanotech Savanah S100 reactor. Most recently, some other reactor designs were analysed by utilizing CFD simulations. Work from Coetzee et al. [117] studied the internal behaviour of a Gemstar 6 square type ALD reactor. In their findings, they discussed the effect of flow in these reactors and the unique buffer layers formed on the substrate surface due to the injection sequence recipe for creating Al₂O₃ thin film. A study from Peltonen et al. [119] studied the Reynolds Number flow effect and injection arrangement that affects the precursor delivery in the Picuson R200 reactor. Their simulations point to the relatively strong variations in the flow fields between low and high Reynolds numbers. By investigation of the flow through their reactor geometry, the study revealed that while the increasing Reynolds number can reduce the required pulse time, no major gain is obtained in the total time sequence of the ALD-cycle. This is due to the purging remaining a slow process, especially in the case of the increased Reynolds number flow nearing turbulence. Additionally, the study confirmed that various reactor specific geometric designs and operating properties, influenced by the different flow patterns observed at different Reynolds numbers, play an important role in the gas flow distribution. However, their study ignored the chemical reaction behaviours at the substrate surface.

A study from Gakis et al. [129] studied the unique flow properties of the Ultratech Fiji F200 reactor. Their model aimed into the investigation of the influence of their reactor geometry and process conditions on the gas flow, temperature fields, and on the species distribution on the heated substrate surface, by neglecting the chemical reactions process at the substrate. The study results illustrated the non-uniformity flow at the pulsing

flow and the purging flow entering the reactor through its loading door that affected the temperature and reactants concentration on the substrate surface.

The substrate topology can be regarded as another critical research domain to understand the flow behaviour across the reactive substrate. However, the topology can cause resistance to uniform deposition film due to the nature of its complex shape. Considering that the future application of ALD would be found within these complex three-dimensional structures, the behaviour and time evolution within these complex topologies could be of great importance. Current studies from the authors [130,131] focus on the development of a fundamental understanding of the mechanistic behaviours within pores and trenches incorporated into the reactive substrate. The author's current studies report on the flow phenomena, mass fraction, surface coverage, deposition rate and conformal growth of Al₂O₃ thin film within trenches along the substrate. One of the studies is to develop model and analyses on the vertical shower head injected type two-dimensional reactors. The purpose of the study is to investigate the mechanistic change of the parameters if a system is operating with and without an additional exposure time. The flow behaviours within and along the trenches are clearly seen and reveal interesting dependent properties to the film growth phenomena. Moreover, the time evolution of the half-reaction surface adsorption process is observed and analysed, along with the major enhancement of the exposure time brings to the ALD process. A study from Olotu et al. [131] revealed the change of the ALD mechanistic behaviour over the previously mentioned substrate and reactor design with the change of pressure. Within his findings, the flow phenomena over the trenches with an introduced exposure time revealed influential mechanistic flow patterns along with different time evolution requirements to create conformal film growth at different pressures. These and future studies are currently being investigated by the authors that incorporate different ALD film recipes, adsorption/desorption kinetics, reactor and substrate mass/fluid flow behaviours, system optimization and the creation of improved ALD processes, among others.

It is worth noting that the analysis technique of the process is scarce in most of the other ALD reactor designs and manufacturers. Due to the different designs of these reactors, future designs in the optimization of the ALD process will need to be similarly investigated to obtain optimal thin film fabrication processes for the numerous types of thin films ALD recipes.

3.2. Experimental methods

ALD grown materials which include oxides, nitrides, sulfides, pure elements and inorganic compounds are realized through the pulse/purge process in ALD reactors. The ALD film deposition methods experimentally depend on the factors such as the nature of the substrate, the deposited materials and the reactor design. The growth rate in ALD is strongly dependent on the aspect ratio of the substrate and the reactor design. Increase in the surface area and volume of an ALD reactor leads to an increase in pulsing and purging time. Substrate structures with high aspect ratio require longer pulsing and purging time for the gases to disperse evenly into the trenches and the three-dimensional features. Spatial ALD was introduced to overcome the longer pulsing and purging time by replacing the pulse/purge chambers spatially revolving heads. This exposes the substrate to a specific gas precursor-based location within the reactor [7]. Numerous reactants/precursors are used in ALD. Non-metal and metal precursors react differently and show different features so are organic compounds [8].

3.2.1. Chemical supply

Wide range of materials can be grown by ALD process. These materials find applications in areas which include semiconductors, metals, insulators, organic and inorganic compounds. Table 6 tabulates materials synthesized by ALD in recent studies based on temperature, film thickness, method and application.

3.2.2. Reactor

Conventional ALD reactors, such as vacuum or viscous flow reactors can be used in ALD for non-planar and high surface area substrates. For the substrates with high aspect ratios, continuous flow processes sometimes require impractical lengths of exposure time for achieving full and uniform fillings of trenches because of the insufficient Knudsen flow of precursor gases. In a stop flow process, higher precursor concentration can be applied since it requires longer diffusion time to deposit on the trench surfaces. When using high-surface-area substrates, it is attractive to use dedicated reactor designs, since the use of conventional reactors will lead to longer deposition times and lower precursor efficiency [64].

Depending on the required deposited materials functionality, there are many different types of ALD reactors such as: batch reactors, compact reactors, fluidized bed reactor, and rotary reactor. The various types of typical ALD reactor systems based on gas injection are (a) Cross-flow reactor system based on forced flow laterally across the wafer, b) system with a single injector above the centre of the wafer, c) showerhead system; gas is injected through an array

of injectors covering the entire wafer surface, and d) vertical batch reactor: 50–150 wafers are processed simultaneously. Table 7 gives ALD reactor types classified by their processing-related characteristics.

3.2.3. Effluent gas handling, emissions, energy consumption

Although ALD has great potentials, yet it has significant sustainability issues that need proper investigation and improvement prior to its full spectrum industrial applications. Among these issues, one of the key problems is the potential nano-particle emissions from the ALD fabrication process which causes occupational, public health risks and environmental impacts due to the unique properties of nanoparticles [166]. Other issues in the ALD process are that only a small percentage of the gases reacts and the greater portion is emitted into the environment [167]. For instance, in the reaction involving TMA, CH₄ (Methane) is emitted, this is not only harmful to the environment but also has an impact on the person(s) handling the experiments. Due to the hazardous nature of TMA, alternative ALD precursors need to be investigated. For example, [3-(dimethylamino)propyl]dimethylaluminium, [AlMe₂(DMP)] (DMAD) [168] has been suggested as ALD precursor that can enable the development of new and promising ALD processes for Al₂O₃ thin films at low temperatures and this finds more applications, nevertheless serious considerations need to be given to the emitted gases. Methane, for instance, has the main impact on a global scale as a greenhouse gas, 21 times more than CO₂. Though its level in the environment is relatively low, it has high global warming potentials.

Yuan et al. [169] performed the sustainability analyses by investigating the film production, precursor emissions, greenhouse gas emissions, and nano-wastes generated quantitatively from the ALD Al₂O₃ processes. They found that huge amounts of environmental emissions are generated which implies that current ALD nanotechnologies need significant improvement before wider industrial applications.

Ma et al. [167] in the emission study of ALD found that it contains 3.22 vol% of CH₄ and 6.01 × 10⁻² vol% of C₂H₆ [167]. They also found that the net peak emissions of the aerosols were between 1 × 10³ and 1 × 10⁴ cm⁻³ and the net total emissions of 25 cycles were in the range of 6.0 × 10⁵ and 2.5 × 10⁶ particles [167]. In an experimental investigation of the emission process in ALD, Ma et al. [170] found that about 93% of trimethylaluminium (TMA) flowed through the chambers without deposition which implies higher emission to the environment. They also reported that 2–9 × 10⁴ of ultrafine nanoparticles containing 51.9 ± 4.6% of C, 16.6 ± 0.9% of Al, 31.4 ± 4.1% of O are generated during each cycle of reactions. They concluded that the purge time has great influence on the ALD emissions

Table 6 Materials grown by ALD process.

Material	Precursor	Purge	Temperature	Film thickness	Method	Application	Ref
TiO ₂	TiIP (Titanium (IV) Ti(CpMe ₅) (OMe) ₃ , O ₃ TDMA, H ₂ O isopropoxide, DI	N ₂ N ₂	90 370 150	103 nm/cycle 0.05 nm/cycle 0.055 nm/cycle	Low-temperature Thermal	Cotton fabrics Capacitor Catalysts membranes, dye-sensitized solar cells, batteries	[132] [133] [134]
SrTiO ₃		O ₃ , O ₂	250–300		Thermal	Capacitor Sensor	[135]
TiO ₂	SO ₂ , [Ecp]Ti(NMe ₂) ₃ Et = CH ₂ CH ₃	Ar	70		Low-temperature	Microelectronics Devices PCRAM	[136]
Ge–Sb–Se–Te (GST)	Sb (OC ₂ H ₅) ₃ and [(CH ₃) ₃ Si] ₂						
SnO _x	Tetrakis(dimethylamino)tin(IV) and H ₂ O	N ₂	80	(0.15 ± 0.01) nm/ cycle	Spatial Atmospheric Pressure Low-temperature	Electronics catalysis Nano wires Carbon separation, capture Solar energy conversion	[137]
SnS ₂	Sn(OAc) ₄ and H ₂ S	N ₂	150–250	0.17 Å/cycle	Thermal Plasma	Solar cell	[138]
TiO ₂	Titanium tetraisopropoxide (TTIP) and H ₂ O	N ₂	200	0.02 nm/cycle		Electronics catalysis Nano wires	[139]
Si-O-Si(CH ₃) ₃	HMDS ((CH ₃) ₃ -Si-N(CH ₃) ₃) + TMCS (Cl-Si(CH ₃) ₃) and H ₂ O	N ₂	180			Carbon separation, capture	[140]
Sb ₂ Se ₃ , TiO ₂ and Pt	Titanium(IV) tetrakisopropoxide (TTIP), and H ₂ O	N ₂	160			Solar energy conversion	[141]
Al ₂ O ₃ and TiO ₂	TiCl ₄ , TMA, OH, O ₂				Low-Temperature	Filtration, gas storage, and catalysis Nano-electronic devices	[142] [143]
Al ₂ O ₃	[Al(NMe ₂) ₂ (DMP)], [Al(NEt ₂) ₂ (DMP)] [Al(NPr ₂) ₂ (DMP)], H ₂ O	N ₂	100 and 180		Thermal and plasma ALD	Microelectronics, organic electronics, solar cells	[168]
V ₂ O ₅	Vanadium triisopropoxide (VTP)	N ₂	150 to 300		Thermal	Capacitors	[202]
Ru	Ru(DMBD)(CO) ₃ and O ₂	N ₂	290 to 320	0.067 nm/cycle	Thermal	Transistors, capacitors	[144]
RuO ₂	Ru(DMBD)(CO) ₃ and O ₂	N ₂	220 to 240	0.065 nm/cycle	Thermal	Transistors, capacitors	[145]
MoS ₂	Mo(NMe ₂) ₄	N ₂	60	1.2 Å/cycle	Thermal	Catalysis, battery	[146]
CuSbS ₂	CuAMD, SbTDMA, H ₂ S	N ₂	225		Low-Temperature	Photovoltaics	[147]
TiO ₂	TiCl ₄ , H ₂ O	N ₂	180	0.6 Å/cycle		Photocatalysis	
TiO ₂	TiCl ₄ , H ₂ O	N ₂	40–250	0.048 nm/cycle to 0.113 nm/cycle	PEALD, tALD	Catalysis, semiconductors	[148]
V ₂ O ₅ and VO ₂	VO[O(C ₃ H ₇) ₃] H ₂ O	N ₂	135	0.03 nm/cycle	PEALD, tALD	Microelectronics	[149]
Ag	Ag(fod) (PEt ₃), BH ₃ (NHMe ₂)	N ₂	110	0.3 Å/cycle	Thermal		[150]
Bi ₂ O ₃	Bi(Ph ₃) ₃ and O ₃	N ₂	250 and 320	0.23 Å/cycle		Supercapacitors, gas sensors, solid oxide fuel cells	[151]
ZnS	ZnS(g-C ₄ N ₄	N ₂	200			Photocatalysis	[152]
Ta ₂ O ₅	Ta(N ^t Bu)(NEt ₂) ₃ , Ta(N ^t Bu)(NEt ₂) ₂ Cp	N ₂	250–300	0.77 and 0.67 Å/ cycle	Thermal	Capacitors, solar cell	[153]
Cobalt ZnO/ZrO ₂	bis(14-di-tert-butyl-1,3-diaza dienyl) cobalt and <i>tert</i> -butylamine (DEZ) and H ₂ O	N ₂ Ar	170 and 200 200	0.98 Å/cycle 1.0 Å/cycle	Low temperature Thermal	Microelectronics Optical and electronic devices	[154] [155,156]
HfO ₂	Tetrakis(ethylamino)zirconium (TEMAZ), diethylzinc (DEZ) HfCl ₄ and H ₂ O	N ₂	200–275	–0	Thermal	Transistors (MOSFET)	[157,158]
HfO ₂	Tetrakis(dimethylamino)hafnium (TDMA-Hf, [(CH ₃) ₂ N] ₄ Hf) and H ₂ O	N ₂	250		Thermal	Microelectronics	[159]
ZnO ₂	(C ₅ H ₅) ₂ Zn [N(CH ₃) ₂] ₃ and O ₃	Ar	180	0.8 Å/cycle	Thermal	Capacitors (DRAM)	[199]
ZnO ₂	CpZn[N(CH ₃) ₂] ₃ C ₇ H ₈ and O ₃	Ar	250 to 350		Thermal	Microelectronics	[160]
ZnO	(C ₂ H ₅) ₂ Zn and H ₂ O	Ar	100 to 300		Plasma, Thermal	Microelectronics, Solar energy	[161– 163]
MoS ₂	Trimethylaluminium (TMA) and H ₂ O	N ₂	200	1 Å/cycle	Thermal	Field-effect transistors (FETs)	[164]

Table 7. Main ALD reactor types classified by their most important processing-related characteristics. (Adapted with permission from [165]).

Reactor	Processing ability	Gas-solid contact	Agglomeration prevention	Energy Provision	Vacuum quality
Flow-type	Medium	Flow through	None (static bed)	Thermal	Medium
Viscous flow	Low	Flow over	None (static bed)	Thermal	Medium
Fluidized bed	High	Mixed flow	Mechanical & pneumatic vibration, stirring, microjet, pulsed flow	Thermal	Medium-atmosphere
Rotary	Medium	Mixed flow	Rotational agitation	Thermal & plasma	High-medium
Pneumatic conveying	High	Local mix (jet)	None	Thermal	Atmospheric

because the purge time changes the reaction as well as the degree of gas phase mixing.

Louwen et al. [171] in their work on the life cycle greenhouse emission and energy payback time of current and prospective heterojunction solar cell designs; compared the ALD with other deposition techniques like the PECVD and the results are presented in Figure 7. The energy consumption of ALD equipment (expressed per m² cell produced) is almost 90% lower according to the equipment data they reviewed. They concluded that ALD has a lower carbon footprint due to plasma enhanced deposition and lower cumulative energy demand. The vacuum operation that could contribute to high energy requirement and carbon footprint is also reduced for this design because the startup of the PECVD equipment (creating vacuum and preheating) is more energy intensive.

ALD design process can be significantly challenging for the chamber exhaust pumps. The chamber exhaust sends the effluent gases to the fab scrubbers. The exhaust system is responsible for making sure the two precursors only interact on the substrate surface and not on the chamber sidewalls and in the exhaust system itself. If this is not properly considered in the design phase, it could become an issue. To prevent this issue, it is necessary to increase the pump speed and separate the two precursor materials [172]. For safety purpose, pump exhaust gases must be appropriately treated before releasing them to

the environment which should be properly incorporated in the design and fit for the purpose.

4. Applications

4.1. Microelectronics

4.1.1. Electronics applications

As technology advances, devices were pushed towards scaled down into nano and atomic levels with more spatially distributed structures. ALD holds the potentials and advantages over other thin film deposition techniques such as CVD and PVD techniques, because of its conformality, composition and control over material thickness. Some of the characteristics of ALD that makes it a tool for nanotechnology includes: atomic scale thickness control, excellent conformality and low growth temperature [5,7]. In this work, few works on the applications in microelectronic materials have been reviewed, as follows.

4.1.2. Transistors

Developing a high ordered three-dimensional structure which provides higher surface area and consequently improving the device efficiency is a growing trend. As a result, the value of the ALD technique has been increased and the presence of ALD in manufacturing semiconductor devices will continue to

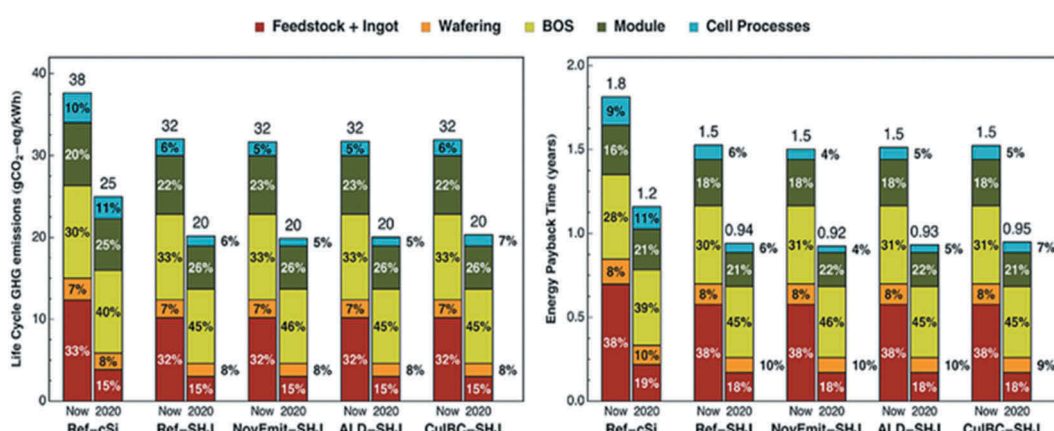


Figure 7. Life cycle greenhouse gas emission and cumulative energy demand in an ALD process compared to other processes. Adapted with permission from [171]. Results are modelled based on cell efficiencies of 20.4% and 25% for current and prospective cells, respectively. SHJ - Silicon heterojunction.

increase. In the recent fabrication of transistors, the research and development are more on the use of ALD for the deposition of conformal films with well-controlled thickness, pinhole-free and high dielectric constant [7]. Several researchers have published works on the use of low-temperature ALD reactor in fabricating the transistors [173–178]. Jin et al. [179] reported the use of ALD for compositional tuning of a range of $Mg_{1-x}Zn_xO$ to fabricate thin film transistors and also the influence of varying the composition and ratios of the oxides on the material and device characteristics. Liu et al. [180] used ALD method to deposit zinc oxide on graphene for thin film transistor. They had a high ON/OFF ratio while the thin film transistor of the zinc oxide on graphene showed enhanced carrier mobility over zinc oxide thin film transistor. In the fabrication of high performance p-type thin film transistors using ALD on silicon oxide films, Kim et al. [181] operated the reactor temperature at 210 °C to suppress the hole carrier concentration effectively. This gave a high ON/OFF ratio and high field-effect mobility though defects and hole carriers. The post-deposition process back channel surface passivation with ALD grown Al_2O_3 at 250 °C post-annealing reduces the defects considerably leading to a superior thin film transistor performance. Figure 8 gives an illustration of ALD application in a transistor. Figure 8(a) shows a traditional planar metal-oxide-semiconductor-field-effect transistor (MOSFET) design while Figure 8(b) shows Fin field effect transistor (FinFET) or trigate design which has been enhanced using the process of ALD. The Si fin which is covered by the gate oxide on three sides is inverted therefore increasing the overall surface area compared to the traditional MOSFET design as shown in Figure 8(a).

In microelectronic industry emerging applications for microelectronic and semiconductor industry in

very large-scale integrated circuit technology are being developed. Figure 9 shows the CVD and ALD process with respect to gas flow sequence. The flow sequence and the expected film growth profiles vs. process time are shown in Figure 9. The deposition rate is continuous for the CVD while the ALD is a cyclical deposition in which the half cycle is self-limited due to the surface chemistry.

More information on the influence of the composition of materials on devices and the effects of temperature transistors through the application of the ALD process can be found in the papers referenced [182–193].

4.1.3. Capacitors

Atomic layer deposition on porous alumina membranes promises a path to produce high-performance capacitors [195]. Groenland et al. [196] studied metal insulator silicon (MIS) and metal insulator metal (MIM) capacitors using titanium nitride. They applied the atomic layer deposition process in the integration of conductors on insulation materials. Further research was done by Dustin et al. [197] used the PEALD to develop Al_2O_3/SiO_2 based metal-insulator-metal-capacitors. They employed the cancelling effects between positive quadratic voltage coefficients of capacitance (αVCC) of aluminium oxide Al_2O_3 and the negative quadratic voltage coefficients of capacitance (αVCC) of silicon oxide (SiO_2). With mainstream materials and low processing temperature, they achieved better leakage current density, capacitance density and voltage nonlinearity [197,198]. More researches have been published on metal-insulator-metal capacitors using ALD [198–201]. More work on the application of ALD for capacitors has been done by different researchers looking at the growth rate, limitations and various applications on different materials [202–207].

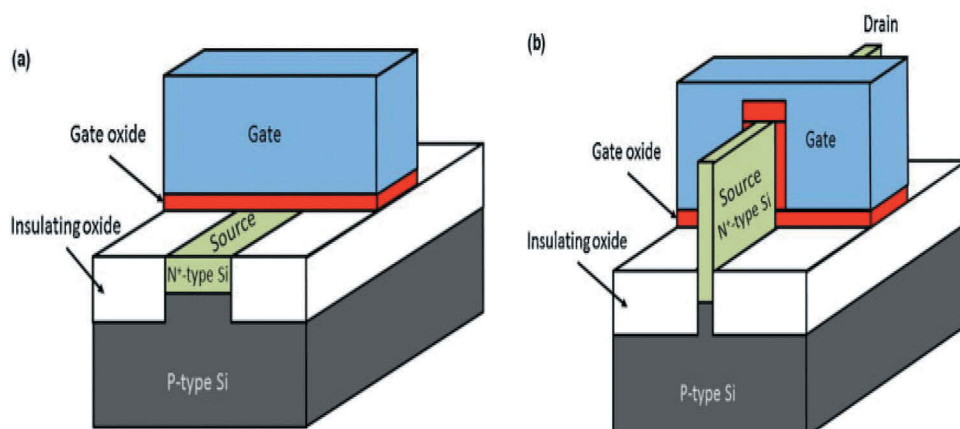


Figure 8. (a) The traditional planar MOSFET design leading to an inverted surface channel and (b) the FinFET or trigate design where a Si fin that is covered by the gate oxide from three sides becomes inverted from the surrounding gate oxide, thus increasing the overall inverted volume compared to the planar design for the same gate voltage. Adapted with permission from [7], copyright Sciedencedirect 2014.

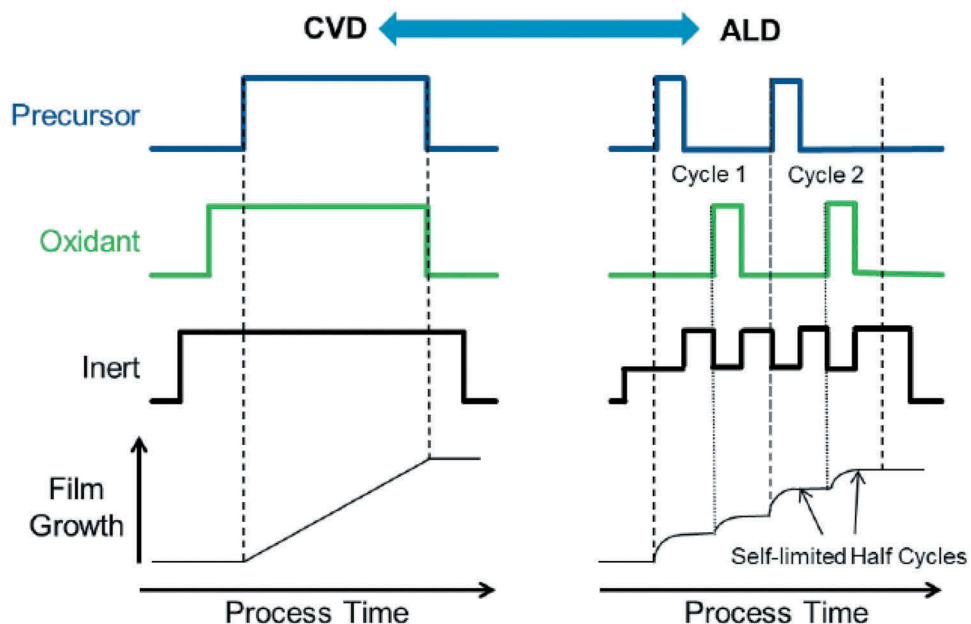


Figure 9. Schematic showing a basic gas flow sequence for Chemical Vapour Deposition (CVD) and for Atomic Layer Deposition (ALD) as well as expected film growth profiles vs. process time. Adapted from [194].

Figure 10 illustrates the new 10-nm-class Dynamic random-access memory (DRAM) with high performance and reliability developed by Samsung. The DRAM which is an 8 Gb (gigabit) chip has more than 8 billion cells. Each of the cells in the chips consists of a capacitor that stores data in the form of electrical charge and the transistor that controls access to it. ALD was applied to achieve this feat that enhances system performance.

4.2. Energy storage and conversion

Fuel cell technology is a promising and reliable clean energy technology due to their low emission of pollutants and high energy conversion efficiency [23]. Among the fuel cell types are polymer electrolyte membrane fuel cells (PEMFCs), direct methanol fuel cell (DMFCs), molten carbonate fuel cells (MCFCs),

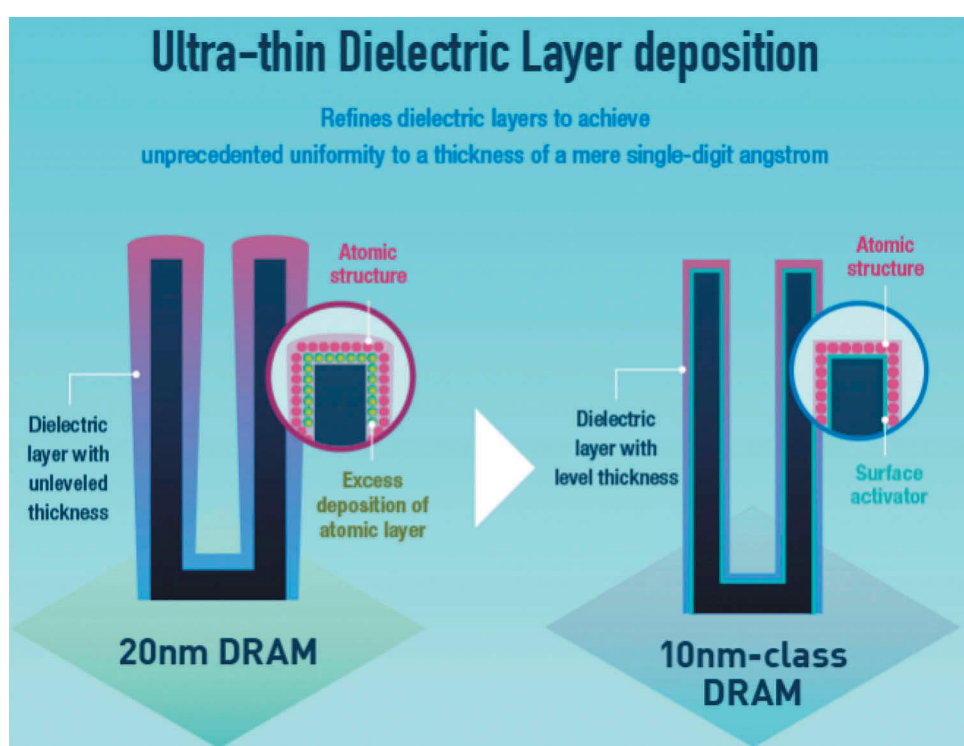


Figure 10. The new 10 nm-class DRAM with high performance and reliability by Samsung. The thickness of the dielectric layers uniform to a few angstroms-DRAM chip contains hundreds of millions to billions of cells depending on data capacity. Each cell consists of two parts: a capacitor that stores data in the form of an electrical charge, and a transistor that controls access to it. Adapted from [208].

solid oxide fuel cells (SOFCs), reversible fuel cell, phosphoric acid fuel cells (PAFCs) and alkaline fuel cells (AFCs). **Introduction of ALD to this field could significantly lower the costs of fuel cells and increase the life-span of the fuel cells.** Catalysts as a part of fuel cells are a major contribution to both the high cost and limited durability of fuel cells [23]. In catalysis, the larger surface-area-to-volume ratio is required therefore particles has preference compared to films. As a common example is to improve the catalytic activity and performance of Pt electrode in fuel cells which can be achieved by modifying the catalytic layer. ALD could be introduced to effectively address the earlier challenges encountered such as high Pt loading, conformity and durability and also could improve the design of the catalysts [209].

Lu et al. [211] reported in porous alumina protective coatings of palladium from poisoning by applying atomic layer deposition as shown in **Figure 11(a)**. They sought to understand how the catalytic activity of the Pd nanoparticles was maintained after ALD of Al_2O_3 cycles expected to bury the Pd nanoparticle surface and concluded that conformal Al_2O_3 films on the Pd nanoparticle surface were achieved.

Jiang et al. [212] created a thin hydrophilic silica aperture at the mouth of the pores, using plasma-directed atomic layer deposition (PD – ALD). **Figure 11(b)** illustrates a cross-sectional schematic of a single membrane before and after the application of catalyst on its surface. The chromium/gold layers already deposited on both sides of the die are used as current collectors. The catalyst layer overlaps with the

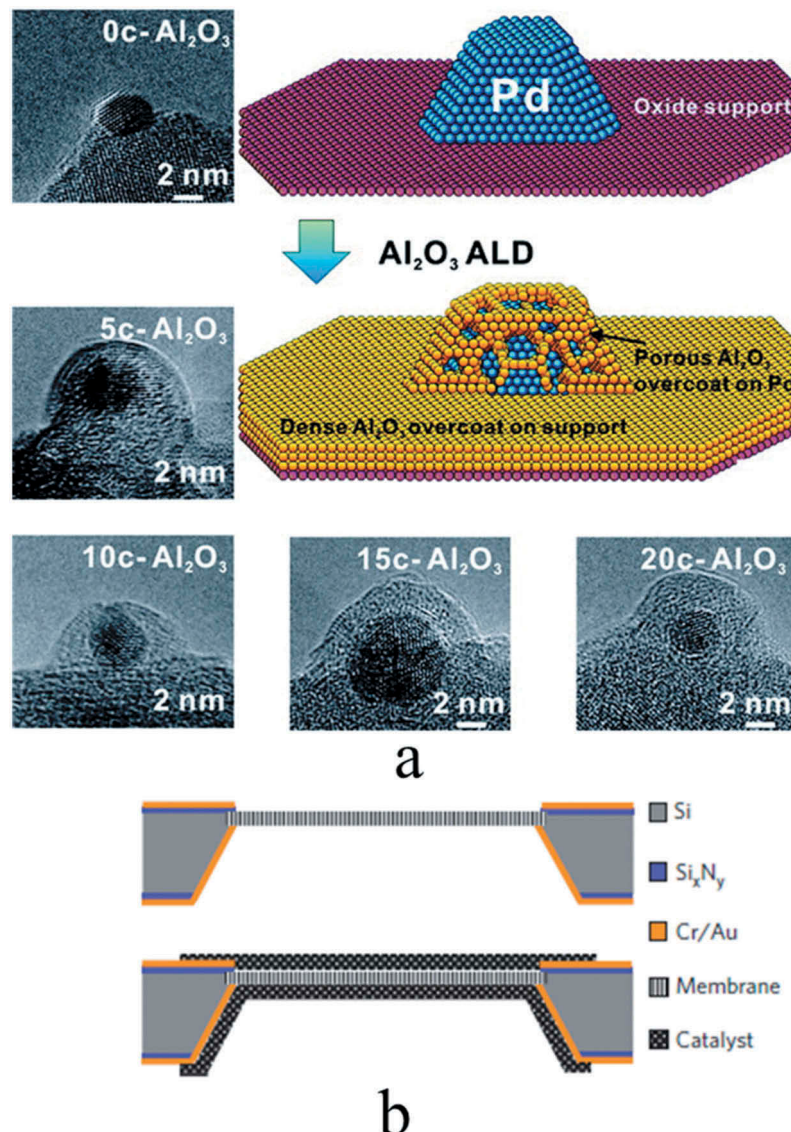


Figure 11. (a) TEM images of spherical alumina supported Pd catalysts with different numbers of Al_2O_3 ALD overcoating from 0 to 20 cycles and schematic illustration of porous ALD Al_2O_3 overcoat on Pd NP for Oxide-supported Pd catalyst and dense Al_2O_3 film on oxide support and porous Al_2O_3 overcoat on Pd NP formed by ALD. Republished with permission from [211], copyright 2012 American Chemical Society, b) Cross-sectional schematic of a single membrane within its silicon die before and after application of the catalyst layers using ALD. Adapted with permission from [210], copyright Nature 2010.

chromium/gold electrode around the edges of the membrane and provides electrical connectivity. The ability to modify the surface of stable membrane enabling the development of better fuel cells.

4.3. Desalination

Freshwater can be obtained from the ocean, sea and brackish waterbodies through the desalination process. However, this process can be costly. In another hand, seawater accounts for about 97.5% of the water resources on earth [213]. Desalination has become increasingly significant for water production in semi-arid coastal areas [214,215]. It is no gainsaying that the world's growing population would need this water source to meet its growing demands. Several technologies are being used in the desalination process, the most desalination technologies at present are based on membrane separation through the reverse osmosis (RO) and thermal distillation (multistage flash (MSF) and multi-effect distillation (MED)) [216]. Reverse osmosis based on polymeric membranes has several challenges which include slow water transport and tremendous energy costs [109,217,218]. Hence, the need for a method to resolve this issue and biomimetic membranes. An emerging technology has promising potentials to address the issues. This review paper will focus on the latest development of biomimetic based membranes.

4.3.1. Biomimetic membrane

Learning from nature has become a common philosophy among the technical and scientific communities. Biomimetic means the study of structures and the functioning of biological systems and developing the model for the design of engineering solutions [219]. Bio-inspiration and biomimetic are now used in many fields such as chemical, materials science, pharmaceuticals, the medical fields, carbon capture and clean energy [220,221]. Different methods have been used in functionalizing a variety of materials for this purpose [222]. According to Zhao et al. [220], ideally biomimetic and bioinspired membranes should possess the following features:

- Fabrication of the membrane through self-assembly under conditions close to the natural atmosphere such as atmospheric pressure, room temperature and aqueous environment.
- The membranes are materials with excellent hydrodynamic, mechanical, wetting and adhesive properties usually composed of the lightest elements in the first two rows of the periodic table.
- The hierarchical organization of the membrane structure spans from molecular-nanoscale-microscale-macroscale bearing controlled configuration, mutable surface and robust interface.

- The membrane properties are highly dependent on the content and state of water in the structure, and membrane processes can be intensified by rationally manipulating the multiple selectivity mechanisms.

Currently, researches are ongoing on ways to integrate high performance bioinspired and biomimetic membranes in industrial and municipal water treatment, but membrane fouling is of great concern in the implementation of membrane water treatment because it increases cleaning requirements, energy consumption and drastic flux decline. The biomimetic membrane can introduce better strategies in developing a range of antifouling membranes which have potentials for better separating capability [221].

Aquaporin which has high water permeability and high solute rejection have attracted interest as functional building blocks for biomimetic membranes in water desalination and water reuse [36].

Susan and team in the Sandia laboratory patented a filter designed mimicking nature (Biomimetic) with porous membranes with controlled nanopores architecture and controlled chemistry through ALD [37,38]. In their work, they developed a biomimetic membrane for water desalination by using ALD technology. The ALD based biomimetic membranes which are centred on selective water transport and solute rejection demonstrate higher water flux and more efficient than commercial membranes available.

The biological aquaporin protein channel – a cellular membrane found in the kidney and other cells, with water transport rates of 10^9 per pore per second with the complete rejection of ions are shown in Figure 12 (left). This provides a working example of a membrane pore that demonstrates fast water flux and selective ion rejection through nanopores at low applied pressure than current reverse osmosis membranes. It shows the complex structural features of the biological pores, short narrow passageway for water and the repulsive hydrophobic walls and the staircase of stabilising polar groups.

Figure 12 further shows a series of *hydrophilic* carbonyl oxygens and amine groups that form a staircase along the other side which is part of the biological filtering mechanism and model for the selective desalination process. Representative snapshot of the silica pore simulated is shown in the right diagram of Figure 12. The Silicon (Si) atoms are coloured orange, the oxygen (O) atoms of silica are coloured red, the Carbon (C) atoms of the methyl groups are coloured green, the Oxygen (O) atoms of the water molecules are coloured blue, and all Hydrogen (H) atoms are coloured white. The simulated system was studied, and the membrane synthesized applying the several methods such as self-induced evaporation and ALD to achieve a membrane with high permeation and better salt rejection.

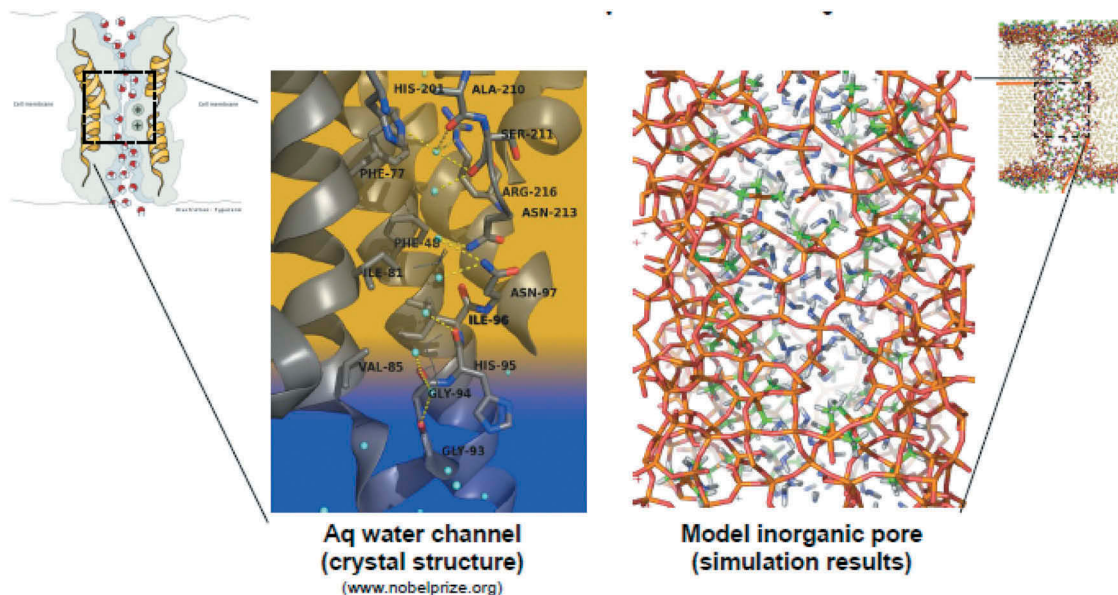


Figure 12. Complex structural features of biological pores that can be adapted for biomimetic filtration. Adapted from [38].

With the system (desalination using ALD tuned membranes), lower energy cost reduction of about 88% and high filtration can be achieved [38]. Two important factors that define the effectiveness and performance of a water desalination membrane are ion rejection and water flux which can be addressed effectively through the ALD process.

ALD, a self-limiting step by step ultra-thin deposition process, was applied in the synthetic nanoporous biomimetic membrane as shown in Figure 13. The channel which is 2.6 nm diameter was functionalised using polypeptides resulting in *hydrophobic* and

hydrophilic functionality in the pore active through the plasma enhanced ALD process. As a result, a small narrow constriction is formed near the surface which rejects Na^+ and Cl^- but allows water to pass through.

Membranes which could include nanoporous materials can be formed through an evaporation-induced self-assembly process forming uniform pore sizes [223,224]. The porous materials could be further tuned to mimic the architecture and chemistry of the biological system hence attain the desired chemical and selective chemical giving the required flux that

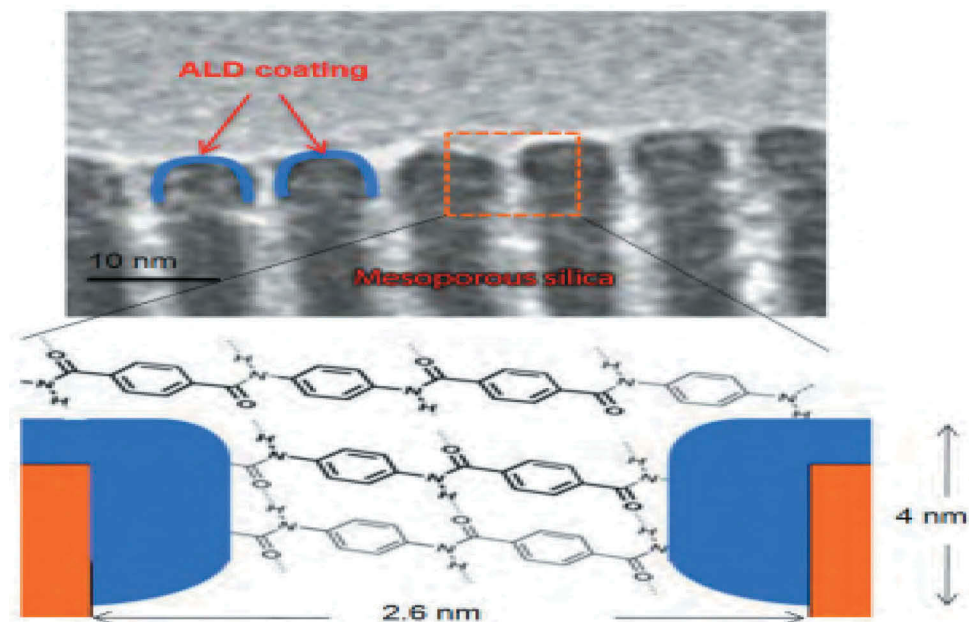


Figure 13. Translated biomimetic design transmission electron microscopy (TEM) showing pore geometry modifications achieved by atomic layer deposition targeted to the pore mouth. ALD of polypeptide groups which modifies internal pore chemistry to produce pore active sites with dimensions and chemical functionality similar to natural biological pores. Adapted from [38]. (Pictures taken from Sandia laboratory publication Biomimetic membrane for water purification 2010 [38]).

the natural biological system possesses. Figure 13 shows the translated biomimetic design transmission electron microscopy (TEM) showing pore geometry modifications achieved by atomic layer deposition targeted to the pore mouth. The support was formed from anodized alumina in this instance but could also be polymers (polysulfone, polyamide, and polycarbonate), ceramics, cermets, metals, alloys, glass and carbon. For water permeation, the pore radius should be equal to or greater than about 0.14 nm after functionalization [38,223]. The functionalised surface could be of amines, carboxylates, nitrides and nitriles; in Figure 13 the as bridged material achieved through ALD, is silsesquioxanes $(RO)_3S - R' - Si(OR)_3$ where R is typically an alkyl group and R' and organic ligand including methane (CH_2), ethane (C_2H_4), phenylene, resulting in a hybrid organic-inorganic material.

Desalination with aquaporin-based bio-inspired membranes holds great potentials compared to current water filters; however, it still has not been fully developed for industrial application partly due to the stability of the membranes during real operations. Only a few studies [37,38,225–228] have been done on biomimetic membranes. However, despite the difficulties, this type of membrane holds great potentials in more productive and sustainable water treatment for solving the water crises in the area where they have saline water. Substantial progress in the permeability of solute-rejecting membranes would mean a great step in improving the economics of desalination for drinking water applications. There are open doors for further research to develop the biomimetic membranes on alternative flexible supports to enable scale-up with temperature, fouling chemical attacks, mechanical stability and pressure effects in perspective which ALD can be an alternative to overcome the constraint of membrane film development.

4.3.2. Graphene

Graphene which is a two-dimensional material with extraordinary properties finds application for many optical and electronic devices and a future for nanoelectronics and many nanotechnology applications. In addition, it has mechanical properties which are good for nanomechanical systems, transparent and conductive composites and thin film transistors [229]. Graphene has high charge carrier, good thermal conductivity, large maximum current density and good light absorbance over broad spectra [230]. Significant development has been made in preparation of large-area graphene. Graphene with very high intrinsic charge carrier mobility (more than $200,000\text{ cm}^2/\text{Vs}$ at 4.2 K) and thermal conductivity above $2000\text{ W}/(\text{m.K})$ at room temperature has become the promising material for electronic and optical applications [230,231].

Integration of graphene in microelectronics devices requires the deposition of thin dielectric layers on top of graphene which brings the challenge. Thanks to the good deposited ultrathin layers of ALD, which generate high-quality films with sub-monolayer thickness control [230]. Wang et al. [232] created an ultrathin film based on aluminium oxide of ALD on graphene. The film which is mechanically robust, pinhole free and thickness in nanometre, and has Young's modulus of $154 \pm 13\text{ GPa}$. These films can be integrated with graphene or other nanomechanical structures to create multi-functional electromechanical structures. They find applications in fields such as thin film coatings, membranes and flexible electronics. The schematic of the graphene membrane before ALD and the optical image after cycles of ALD with the atomic force microscope images is shown in Figure 14.

According to Alles et al. [233], for the ALD of high-quality dielectric layers, a seed layer is grown using highly reactive precursors and low deposition temperature or through functionalization of the graphene surface with a metal or polymer buffer layer. However, this could lead to degradation of the electronic properties of graphene or result in a higher high-k dielectric layer. It has been suggested that further experiments are required for the optimization of the graphene parameters to derive its full electronic potential.

Owing to the exceptional properties of graphene, it finds many applications and has the potential to address the issues of water desalination and climate change. Cohen-Tanugi et al. [96,234,235] demonstrated this through their simulation work on desalination using graphene membranes as a function of pore size, chemical functionalization and applied pressure to effectively address the high energy required in the reverse osmosis system. The pore size and surface chemistry functionalized through hydrogenation and hydroxylation are shown in Figure 15. The fabrication can be effectively done through the ALD process. In mimicking nature for the water transport, graphene oxide membrane was functionalized with aquaporin-mimicking peptides [236]. Even though it is not through the ALD process, a similar result was achieved compared to the result from Sandia laboratory which is through the process of ALD [38].

4.4. Catalyst

Catalysis is an essential technology for accelerating and directing chemical transformations. ALD is a powerful tool for atomically precise design and synthesis of catalytic materials. It is key to develop new technologies in creating values from sources such as fossil fuel, biomass, carbon dioxide and water. It finds application in major

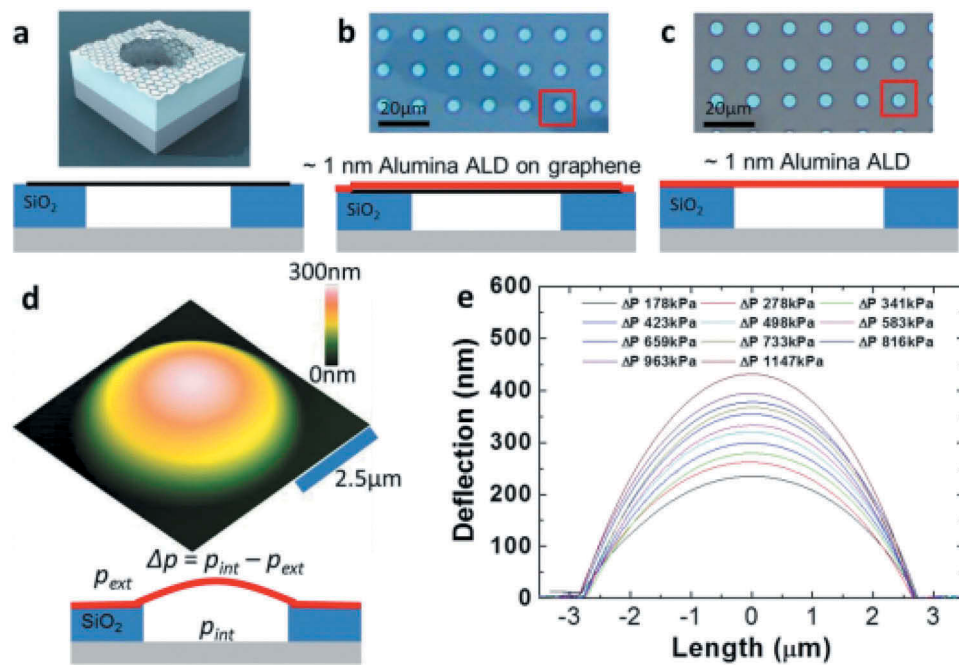


Figure 14. (a) Schematic of a graphene membrane before atomic layer deposition (ALD). (b) Optical image of an exfoliated graphene flake with 7 cycles of alumina ALD. (c) Optical image of a pure alumina film after graphene is etched away. (d) Atomic force microscope image of a pressurized 7-cycle pure alumina ALD film with $\Delta p = 278 \text{ kPa}$. (e) Deflection vs. position through the centre of the film in (d) at different Δp . Adapted with permission from [232], copyright Nanoletters 2012.

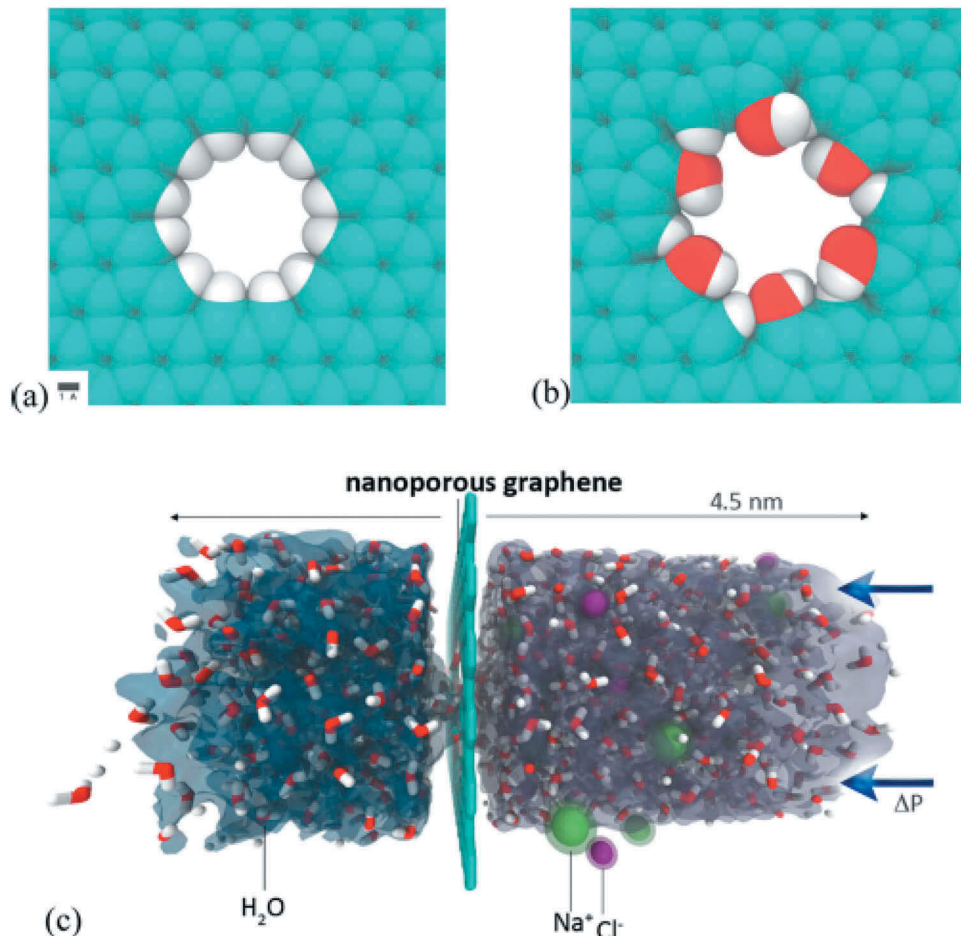


Figure 15. (a) Hydrogenated graphene pore (b) and hydroxylated graphene pore, and (c) side view of the computational system. Adapted with permission from [228], copyright Nanoletters 2012.

industries such as energy, pharmaceuticals, healthcare, chemicals, agriculture, food processing, consumer products and environmental remediation [237]. The grand challenge is how to improve the selectivity of catalysts to convert the specific feed to specific products with little or no waste in conjunction with undesirable reactions.

The task of simultaneously improving catalytic activity, selectivity and stability are common for both organic and inorganic catalysts, and a central goal is to control the size, shape, and morphology of supported nanoparticles to improve selectivity. Tailoring catalysts with atomic-level control over active sites and composite structures are of great importance for advanced catalysis [238]. Figure 16(a) shows the preparation of core-shell nanoparticles with three strategies and their

applications through ALD include the core-shell structures, discontinuous coating structures, and embedded structures. ALD has been shown to be effective at controlling metal and metal oxide active sites and improving catalytic activity, selectivity, and longevity. More importantly, ALD is an effective method in making uniformly dispersed catalyst on large surface area supports. Putkonen et al. [239] studied the effect of ALD on the improvement of other methods to fabricate good performance catalyst in the Fischer-Tropsch process. They showed that combining ALD with washcoating method for catalyst preparation resulted in a highly active catalyst. This comparison is illustrated in Figure 16(b). The Fischer-Tropsch process uses a collection of chemical reactions to convert mixtures

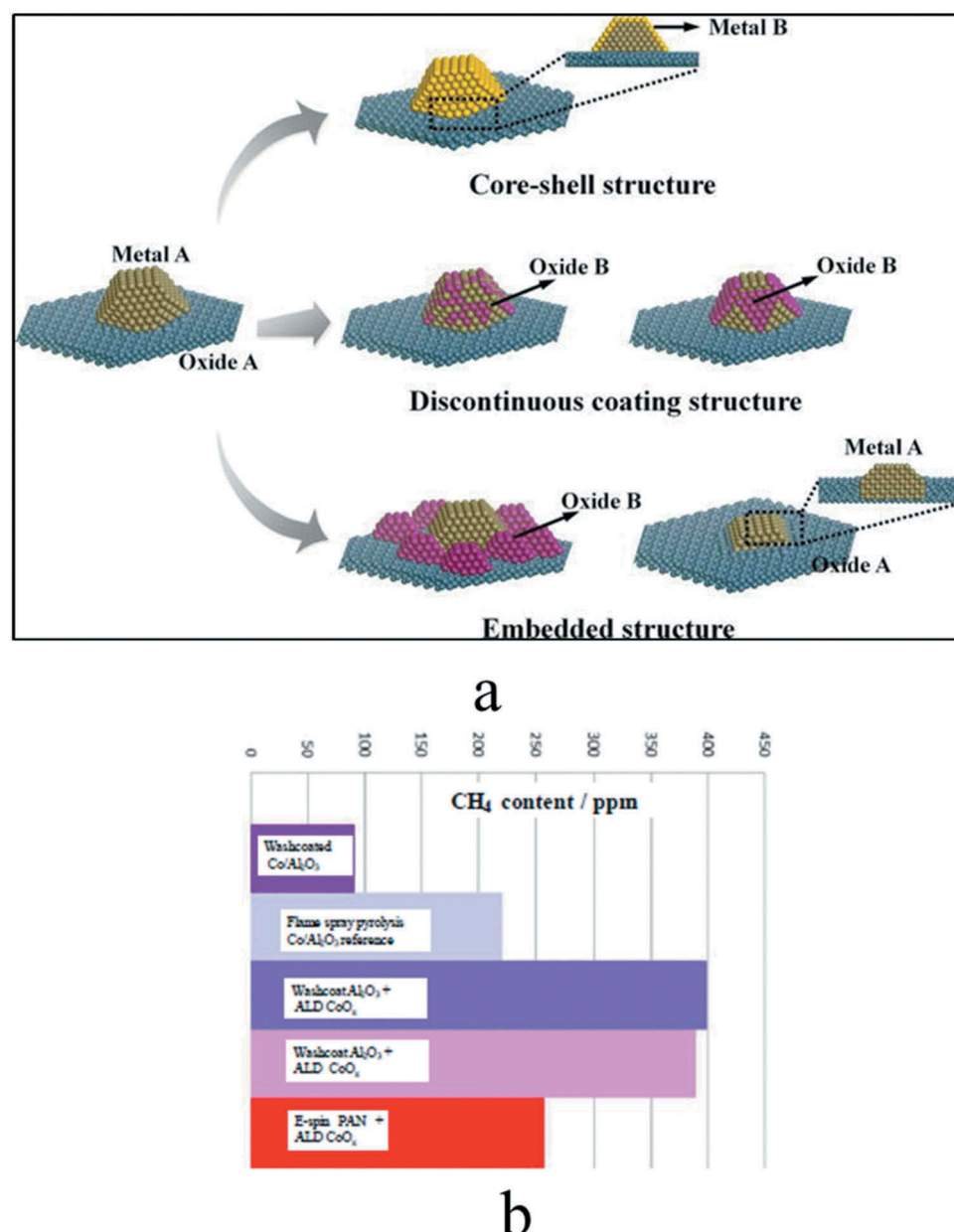


Figure 16. (a) Classification of composite catalysts synthesized with selective ALD in this review, (I) core-shell structure, (II) discontinuous coating structure, and (III) embedded structure. Republished with permission from [238], copyright 2017 Author(s). (b) The effect of different catalysts on Fischer-Tropsch synthesis CH₄ output measured by Gas Chromatograph (Adapted with permission from [239]).

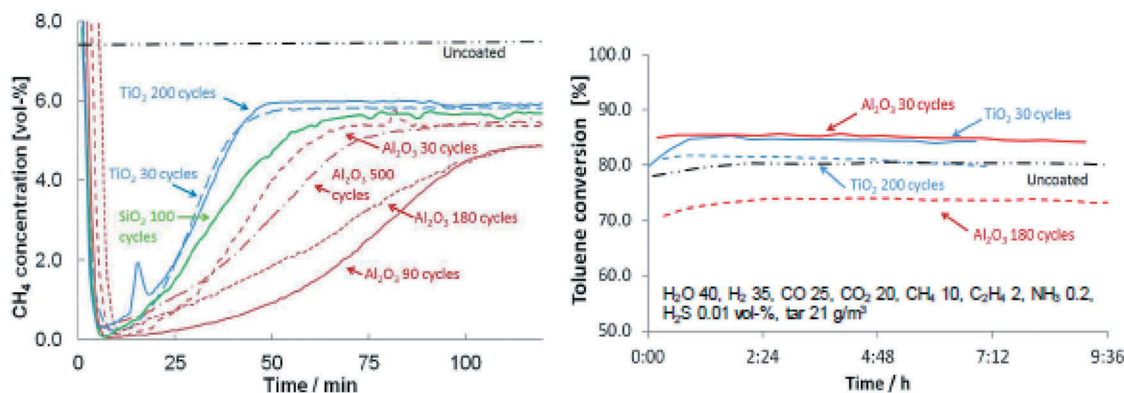


Figure 17. The effect of ALD oxide layers on the commercial nickel-based catalyst (left) and on commercial noble metal catalyst (right) activity on steam reforming (Adapted with permission from [239]).

of hydrogen and carbon monoxide into liquid hydrocarbons. The Fischer-Tropsch process is now a method of choice for the synthesis of petroleum substitutes. The highest activity was obtained with metal plates having Al₂O₃ by the washcoating method and CoO_x by ALD which clearly shows the positive influence of ALD.

They also prove that ALD overcoating could suppress the commercial catalysts deactivation which happens during steam reforming, especially by thin Al₂O₃ layers.

In an attempt to synthesize some organic catalysts, the effect of the application of ALD for catalyst preparation was evaluated. In this study, the efficiency of CH₄ and toluene conversion was studied using thin film catalyst and the effect of the number of film layers created by ALD was compared. As it can be seen from Figure 17, there was a difference in the product conversion for methane, ethylene and toluene with noble metal catalysts where ALD was used to prepare the catalyst with different thicknesses. Thinnest ALD coating had the highest improvements which show the ability of ALD in fabricating thin film.

To further demonstrate the growing application of ALD, a group of scientists developed a testing tool – integrated atomic layer deposition synthesis-catalysis (I-ALD-CAT) for catalyst synthesis and performance evaluation of a catalyst. It combines an ALD manifold with a plug flow reactor system. The I-ALD-CAT was successfully used in synthesizing platinum active sites, Al₂O₃ overcoats and in the activity evaluation of propylene hydrogenation under plug-flow conditions [240].

4.5. Medical

Numerous emerging flexible sensing technologies which can be used for many physical and physiological measurements in the medical fields are available [241]. Since the demand for these applications is

increasing so also the processes to get effective ways of implementing them. ALD finds applications in developing some of these materials and devices.

Practically ALD using low deposition temperature has already been used in the manufacturing of flexible organic field-effect transistors (OFETs) [242]. The OFETs find application in transducing mechanical and chemical stimuli into electrical signals [243].

ALD is also finding applications in the fields of plasmonics, nanoscience and nanobiotechnology. The coatings can be used to modify the metallic surfaces and tune the optical and plasmonic properties which protect the surface from oxidation and contamination to create the required biocompatible surface [244].

ALD could also find application in nanostructured materials which are useful for the delivery of a pharmacological agent at a precise rate and specific locations in the body [245]. These nanostructured materials have applications in orthopaedic implants or self-sterilizing medical devices. In a study, Bilo et al. [246] demonstrated that ALD is a suitable coating technique to prevent metal diffusion from medical implants.

ALD has also been used in the design of nanoparticles, and larger-sized, single drug powder particle applications, as well as on tablet formulations [247]. ALD applications in active pharmaceutical ingredients are also being developed (APIs) [248].

5. Conclusions

This research review highlights the importance of atomic layer deposition (ALD) for different applications. ALD is becoming one of the most promising methods for depositing and producing high-quality thin film. It has proven and shown its potential to meet the demand for a variety of applications. Emerging branches of the technology are setting

new opportunities and challenges for ALD processes to meet this continuous expansion of the material selection and divergent needs for conformal, high quality, and ultra-thin films. This study has gathered the information on ALD techniques in both aspects, experimentally and computational, and has compared their pros and cons with other methods. Some of the main drawbacks are the precursor wastage, energy wastage, time required for chemical reactions, nano-particles emissions and the economic viability. The advantages include the film conformity, deposition on challenging substrates, stoichiometric control and the inherent film quality associated with self-limiting, self-assembled nature of the ALD mechanism.

It has also summarized different applications in the selected fields of ALD up-to-date. Finally, this can give good and quick guidance to those researchers and practising engineers who wish to use ALD as the tool form research and engineering applications.

Acknowledgments

The authors would like to acknowledge the financial support from the National Research Foundation (NRF) of South Africa and the Global Excellence Scholarship (GES).

Disclosure statement

No potential conflict of interest was reported by the authors.

References

- [1] Puurunen RL. A short history of atomic layer deposition: tuomo Suntola's atomic layer epitaxy. *Chem Vap Deposition*. 2014;20:332–344.
- [2] Suntola T. Atomic layer epitaxy. *Thin Solid Films*. 1992;216:84–89.
- [3] Li PH, Chu PK. 1 - Thin film deposition technologies and processing of biomaterials. In: Griesser HJ, editor. *Thin Film coatings for biomaterials and biomedical applications*. Duxford (UK): Woodhead Publishing; 2016. p. 3–28.
- [4] Pan D, Ma L, Xie Y, et al. On the physical and chemical details of alumina atomic layer deposition: A combined experimental and numerical approach. *J Vac Sci Technol A*. 2015;33:021511.
- [5] Kim H, Lee H-B-R, Maeng W-J. Applications of atomic layer deposition to nanofabrication and emerging nanodevices. *Thin Solid Films*. 2009 Feb 2;517:2563–2580.
- [6] Miikkulainen V, Leskelä M, Ritala M, et al. ChemInform abstract: crystallinity of inorganic films grown by atomic layer deposition: overview and general trends. Vol. 113. American Institute of Physics; 2013.
- [7] Johnson RW, Hultqvist A, Bent SF. A brief review of atomic layer deposition: from fundamentals to applications. *Mater Today*. 2014;17:236–246.
- [8] Leskelä M, Ritala M. Atomic layer deposition (ALD): from precursors to thin film structures. *Thin Solid Films*. 2002 Apr 22;409:138–146.
- [9] Kwon J, Dai M, Halls MD, et al. In situ infrared characterization during atomic layer deposition of lanthanum oxide. *J Phys Chem C*. 2009 Jan 15;113:654–660.
- [10] Shaeri MR, Jen T-C, Yuan CY, et al. Investigating atomic layer deposition characteristics in multi-outlet viscous flow reactors through reactor scale simulations. *Int J Heat Mass Transfer*. 2015 Oct 1;89:468–481.
- [11] Ram C, Jen TC. Numerical modelling in the atomic layer deposition process: A short review, unpublished.
- [12] Shaeri MR, Jen T-C, Yuan CY. Improving atomic layer deposition process through reactor scale simulation. *Int J Heat Mass Transfer*. 2014 Nov 1;78:1243–1253.
- [13] Yan B, Li X, Bai Z, et al. A review of atomic layer deposition providing high performance lithium sulfur batteries. *J Power Sources*. 2017 Jan 15;338:34–48.
- [14] Kim H. Atomic layer deposition of metal and nitride thin films: current research efforts and applications for semiconductor device processing. *J Vac Sci Technol B Microelectron Nanometer Struct Process Meas Phenom*. 2003;21:2231–2261.
- [15] Kanarik KJ, Marks J, Singh H, et al. Integrating atomic scale processes: ALD (atomic layer deposition) and ALE (atomic layer etch). Google Patents, 2017.
- [16] Kim KH, Gordon RG, Ritenour A, et al. Atomic layer deposition of insulating nitride interfacial layers for germanium metal oxide semiconductor field effect transistors with high- κ oxide/tungsten nitride gate stacks. *Appl Phys Lett*. 2007;90:212104.
- [17] Meng X, Byun Y-C, Kim H, et al. Atomic layer deposition of silicon nitride thin films: a review of recent progress, challenges, and outlooks. *Materials*. 2016;9:1007.
- [18] Kanarik KJ, Lill T, Hudson EA, et al. Overview of atomic layer etching in the semiconductor industry. *J Vac Sci Technol A*. 2015;33:020802.
- [19] Kong X. Atomic layer deposition for photovoltaics: applications and prospects. In: Light, energy and the environment 2015. Suzhou: Optical Society of America; 2015.
- [20] Muñoz-Rojas D, Nguyen VH, Masse de la Huerta C, et al. Spatial Atomic Layer Deposition (SALD), an emerging tool for energy materials. Application to new-generation photovoltaic devices and transparent conductive materials. *C R Phys*. 2017 Sept 1;18:391–400.
- [21] Jung YS, Cavanagh AS, Riley LA, et al. Ultrathin direct atomic layer deposition on composite electrodes for highly durable and safe Li-Ion batteries. *Adv Mater*. 2010;22:2172–2176.
- [22] Meng X, Yang X-Q, Sun X. Emerging applications of atomic layer deposition for lithium-ion battery studies. *Adv Mater*. 2012;24:3589–3615.
- [23] Cheng N, Shao Y, Liu J, et al. Electrocatalysts by atomic layer deposition for fuel cell applications. *Nano Energy*. 2016;29:220–242.
- [24] Jung YS, Cavanagh AS, Dillon AC, et al. Enhanced stability of LiCoO₂ cathodes in lithium-ion batteries using surface modification by atomic layer deposition. *J Electrochem Soc*. 2010 Jan 1;157:A75–A81.

- [25] Ma L, Nuwayhid RB, Wu T, et al. Atomic layer deposition for lithium-based batteries. *Adv Mater Interfaces*. **2016**;3:1600564-n/a.
- [26] Knoops HCM, Donders ME, Sanden MCMVD, et al. Atomic layer deposition for nanostructured Li-ion batteries. *J Vac Sci Technol A*. **2012**;30:010801.
- [27] Wenbin N, Xianglin L, Siva Krishna K, et al. Applications of atomic layer deposition in solar cells. *Nanotechnology*. **2015**;26:064001.
- [28] Pearse AJ, Schmitt TE, Fuller EJ, et al. Nanoscale solid state batteries enabled by thermal atomic layer deposition of a lithium polyphosphazene solid state electrolyte. *Chem Mater*. **2017** Apr 25;29:3740–3753.
- [29] Delft JAV, Garcia-Alonso D, Kessels WMM. Atomic layer deposition for photovoltaics: applications and prospects for solar cell manufacturing. *Semicond Sci Technol*. **2012**;27:074002.
- [30] Schmidt J, Merkle A, Brendel R, et al. Surface passivation of high-efficiency silicon solar cells by atomic-layer-deposited Al₂O₃. *Prog Photovoltaics Res Appl*. **2008**;16:461–466.
- [31] Hoex B, Heil SBS, Langereis E, et al. Ultralow surface recombination of c-Si substrates passivated by plasma-assisted atomic layer deposited Al₂O₃. *Appl Phys Lett*. **2006**;89:042112.
- [32] Palmstrom AF, Santra PK, Bent SF. Atomic layer deposition in nanostructured photovoltaics: tuning optical, electronic and surface properties. *Nanoscale*. **2015**;7:12266–12283.
- [33] Barbos C, Blanc-Pelissier D, Fave A, et al. Al₂O₃ thin films deposited by thermal atomic layer deposition: characterization for photovoltaic applications. *Thin Solid Films*. **2016** Oct 30;617:108–113.
- [34] Jaramillo R, Steinmann V, Yang C, et al. Making record-efficiency sns solar cells by thermal evaporation and atomic layer deposition. *J Vis Exp*. **2015** May 22; (99):e52705.
- [35] Poodt P, Cameron DC, Dickey E, et al. Spatial atomic layer deposition: A route towards further industrialization of atomic layer deposition. *J Vac Sci Technol A*. **2012**;30:010802.
- [36] Tang CY, Zhao Y, Wang R, et al. Desalination by biomimetic aquaporin membranes: review of status and prospects. *Desalination*. **2013** Jan 2;308:34–40.
- [37] Rempe SBR, David M, Jiang Y-B, et al. Computational and experimental platform for understanding and optimizing water flux and salt rejection in nanoporous membranes. Sandia National Laboratories, Albuquerque, NM2010.
- [38] Rempe SB, Biomimetic membrane for water purification, **2011**.
- [39] Simon DE. Atomic-scale simulation of ALD chemistry. *Semicond Sci Technol*. **2012**;27:074008.
- [40] Fu Y, Li B, Jiang Y-B, et al. Atomic layer deposition of L-Alanine polypeptide. *J Am Chem Soc*. **2014**;136:15821–15824.
- [41] Hao W, Marichy C, Journet C, et al. A novel two-step ammonia-free atomic layer deposition approach for boron nitride. *ChemNanoMat*. **2017**;3:656–663.
- [42] Li D, Hu J, Low Z-X, et al. Hydrophilic ePTFE membranes with highly enhanced water permeability and improved efficiency for multipollutant control. *Ind Eng Chem Res*. **2016** Mar 16;55:2806–2812.
- [43] Oviroh PO, Akbarzadeh R, Jen T-C. Biomimetic membrane simulation for water desalination. ASME. ASME International Mechanical Engineering Congress and Exposition, Volume 10: Micro- and Nano-Systems Engineering and Packaging. **2018**;V010T13A003.
- [44] Akbarzadeh R, Ghole VS, Javadpour S. Durable titania films for solar treatment of biomethanated spent wash. *Russ J Phys Chem A*. **2016** October 01;90:2060–2068.
- [45] Akbarzadeh R, Umbarkar SB, Sonawane RS, et al. Vanadia-titania thin films for photocatalytic degradation of formaldehyde in sunlight. *Appl Catal A Gen*. **2010** Feb 1;374:103–109.
- [46] Matsuoka M, Toyao T, Horiuchi Y, et al. Wastewater treatment using highly functional immobilized TiO₂ thin-film photocatalysts. In: Pichat P, editor. *Photocatalysis and Water Purification*. Wiley Online Library; **2013**. p. 179–197.
- [47] Pala A, Politi RR, Öner G, et al. Nanocoating thin film applications on water treatment. *Mater Today Proc*. **2015** Jan 1;2:271–280.
- [48] Zhong Z, Xu Z, Sheng T, et al. Unusual air filters with ultrahigh efficiency and antibacterial functionality enabled by ZnO nanorods. *ACS Appl Mater Interfaces*. **2015** Sept 30;7:21538–21544.
- [49] Feng S, Li D, Low Z-X, et al. ALD-seeded hydrothermally-grown Ag/ZnO nanorod PTFE membrane as efficient indoor air filter. *J Membr Sci*. **2017** June 1;531:86–93.
- [50] Louda P. Applications of thin coatings in automotive industry. *J. Achiev. Mater. Manuf*. **2007**;24:50–56.
- [51] Narayan RJ, Adiga SP, Pellin MJ, et al. Atomic layer deposition-based functionalization of materials for medical and environmental health applications. *Philos Trans R Soc A Math Phys Eng Sci*. **2010**;368:2033–2064.
- [52] Travis C, Adomaitis R. Dynamic modeling for the design and cyclic operation of an atomic layer deposition (ALD) reactor. *Processes*. **2013**;1:128.
- [53] Abou Chaaya A, Le Poitevin M, Cabello-Aguilar S, et al. Enhanced ionic transport mechanism by gramicidin a confined inside nanopores tuned by atomic layer deposition. *J Phys Chem C*. **2013** July 25;117:15306–15315.
- [54] French P, Krijnen G, Roozeboom F. Precision in harsh environments. *Microsys Nanoeng*. **2016** Oct 10;2:16048.
- [55] Nguyen MT, Yonezawa T. Sputtering onto a liquid: interesting physical preparation method for multi-metallic nanoparticles. *Sci Technol Adv Mater*. **2018** Dec 31;19:883–898.
- [56] Yabu H. Fabrication of honeycomb films by the breath figure technique and their applications. *Sci Technol Adv Mater*. **2018** Dec 31;19:802–822.
- [57] Zhuiykov S, Kawaguchi T, Hai Z, et al. Interfacial engineering of two-dimensional nano-structured materials by atomic layer deposition. *Appl Surf Sci*. **2017**;392:231–243.
- [58] Muñoz-Rojas D, MacManus-Driscoll J. Spatial atmospheric atomic layer deposition: a new laboratory and industrial tool for low-cost photovoltaics. *Mater Horiz*. **2014**;1:314–320.

- [59] Bae C, Shin H, Nielsch K. Surface modification and fabrication of 3D nanostructures by atomic layer deposition. *MRS Bull.* **2011**;36:887–897.
- [60] Losic D, Triani G, Evans PJ, et al. Controlled pore structure modification of diatoms by atomic layer deposition of TiO₂. *J Mater Chem.* **2006**;16:4029–4034.
- [61] Zhang Y, Liu B, Hitz E, et al. A carbon-based 3D current collector with surface protection for Li metal anode. *Nano Res.* **2017** April 01;10:1356–1365.
- [62] Kim E, Vaynzof Y, Sepe A, et al. Gyroid-structured 3D ZnO networks made by atomic layer deposition. *Adv Funct Mater.* **2014**;24:863–872.
- [63] Rolison DR, Long JW, Lytle JC, et al. Multifunctional 3D nanoarchitectures for energy storage and conversion. *Chem Soc Rev.* **2009**;38:226–252.
- [64] Bui HV, Grillo F, Ommen JRV. Atomic and molecular layer deposition: off the beaten track. *Chem Comm.* **2017**;53:45–71.
- [65] Napari M. Low-temperature thermal and plasma-enhanced atomic layer deposition of metal oxide thin films. PhD, Department of Physics, University of Jyväskylä, Finland, **2017**.
- [66] Musschoot J. Advantages and challenges of plasma enhanced atomic layer deposition [doctoral dissertation]. Ghent University; **2011**.
- [67] Hyungjun K, Il-Kwon O. Review of plasma-enhanced atomic layer deposition: technical enabler of nanoscale device fabrication. *Jpn J Appl Phys.* **2014**;53:03DA01.
- [68] Musschoot J. Advantages and challenges of plasma enhanced atomic layer deposition, **2012**.
- [69] Heil SBS, Hemmen JLV, Hodson CJ, et al. Deposition of TiN and HfO₂ in a commercial 200mm remote plasma atomic layer deposition reactor. *J Vac Sci Technol A.* **2007**;25:1357–1366.
- [70] Pan D, Ma L, Xie Y, et al. On the physical and chemical details of alumina atomic layer deposition: a combined experimental and numerical approach. *J Vac Sci Technol A.* **2015**;33:021511.
- [71] Shaeri MR, Jen TC, Yuan CY, et al. Investigating atomic layer deposition characteristics in multi-outlet viscous flow reactors through reactor scale simulations. *Int J Heat Mass Transfer.* **2015** June 6;89:468–481.
- [72] Shaeri MR, Jen TC, Yuan CY. Reactor scale simulation of an atomic layer deposition process. *Chem Eng Res Des.* **2015**;94:584–593.
- [73] Pan D. Numerical and experimental studies of atomic layer deposition for sustainability improvement. Doctor of Philosophy in Engineering, The University of Wisconsin-Milwaukee, **2016**.
- [74] Pan D, Jen TC, Yuan C. Effects of gap size, temperature and pumping pressure on the fluid dynamics and chemical kinetics of in-line spatial atomic layer deposition of Al₂O₃. *Int J Heat Mass Transfer.* **2016** January 11;96:189–198.
- [75] Pan D, Ma L, Xie Y, et al. Experimental and numerical investigations into the transient multi-wafer batch atomic layer deposition process with vertical and horizontal wafer arrangements. *Int J Heat Mass Transfer.* **2015**;91:416–427.
- [76] Shaeri MR. Reactor scale simulation of atomic layer deposition. Doctor of Philosophy in Engineering, The University of Wisconsin-Milwaukee, **2014**.
- [77] Shaeri MR, Jen TC, Yuan CY. Improving atomic layer deposition process through reactor scale simulation. *Int J Heat Mass Transfer.* **2014**;78:1243–1253.
- [78] Merchant TP, Gobbert MK, Cale TS, et al. Multiple scale integrated modeling of deposition processes. *Thin Solid Films.* **2000**;365:368–375.
- [79] Gobbert MK, Cale TS. Modeling multiscale effects on transients during chemical vapor deposition. *Surf Coat Technol.* **2007**;201:8830–8837.
- [80] Gobbert MK. A multiscale simulator for low pressure chemical vapor deposition. *J Electrochem Soc.* **1997**;144:3945.
- [81] Gobbert MK, Prasad V, Cale TS. Predictive modeling of atomic layer deposition on the feature scale. *Thin Solid Films.* **2002**;410:129–141.
- [82] Remmers EM, Travis CD, Adomaitis RA. Reaction factorization for the dynamic analysis of atomic layer deposition kinetics. *Chem Eng Sci.* **2015**;127:374–391.
- [83] Jones AAD, Jones AD. Numerical simulation and verification of gas transport during an atomic layer deposition process. *Mater Sci Semicond Process.* **2014**;21:82–90.
- [84] Holmqvist A, Magnusson F, Stenström S. Scale-up analysis of continuous cross-flow atomic layer deposition reactor designs. *Chem Eng Sci.* **2014**;117:301–317.
- [85] Tu J, Yeoh GH, Liu C. Computational fluid dynamics: a practical approach. Butterworth-Heinemann; **2018**.
- [86] Mahajan RL. Transport phenomena in chemical vapor-deposition systems. In: Poulikakos D, editor. *Advances in heat transfer*. Vol. 28. Elsevier; **1996**. p. 339–425.
- [87] Jitschin W, Reich R. Molecular velocity distribution at large Knudsen numbers. *J Vac Sci Technol A.* **1991**;9:2752–2756.
- [88] Gerhart PM, Gerhart AL, Hochstein JI. *Fluid mechanics*. New York (NY): John Wiley & Sons; **2017**.
- [89] Shaeri MR (2014). Reactor scale simulation of atomic layer deposition.
- [90] Yuan J, Sundén B. On continuum models for heat transfer in micro/nano-scale porous structures relevant for fuel cells. *Int J Heat Mass Transfer.* **2013**;58:441–456.
- [91] Quan Liao T-CJ. Application of lattice boltzmann method in fluid flow and heat transfer. In: Minin O, editor. *Computational fluid dynamics technologies and applications*. Croatia: IntechOpen; **2011**.
- [92] Cremers V, Geenen F, Detavernier C, et al. Monte Carlo simulations of atomic layer deposition on 3D large surface area structures: required precursor exposure for pillar- versus hole-type structures. *J Vac Sci Technol A.* **2017**;35:01B115.
- [93] Knoops HCM, Langereis E, van de Sanden MCM, et al. Conformality of plasma-assisted ALD: physical processes and modeling. *J Electrochem Soc.* **2010** December 1;157:G241–G249.
- [94] Shirazi M, Elliott SD. Atomistic kinetic Monte Carlo study of atomic layer deposition derived from density functional theory. *J Comput Chem.* **2014**;35:244–259.
- [95] Leimkuhler B, Matthews C. *Molecular dynamics: with deterministic and stochastic numerical methods*. Cham (Switzerland): Springer International Publishing; **2015**.
- [96] Cohen-Tanugi D. Nanoporous graphene as a water desalination membrane. PhD, Department of Materials Science and Engineering, Massachusetts Institute of Technology, Massachusetts, **2015**.
- [97] Pan D, Li T, Chien Jen T, et al. Numerical modeling of carrier gas flow in atomic layer deposition vacuum reactor: A comparative study of lattice Boltzmann models. *J Vac Sci Technol A.* **2014**;32:01A110.

- [98] Heiranian M, Wu Y, Aluru NR. Molybdenum disulfide and water interaction parameters. *J Chem Phys.* **2017**;147:104706.
- [99] Rapaport DC. The art of molecular dynamics simulation. Cambridge (UK): Cambridge University Press; **2004**.
- [100] Hospital A, Goñi JR, Orozco M, et al. Molecular dynamics simulations: advances and applications. *Adv Appl Bioinf Chem AABC.* **2015**;8:37–47.
- [101] Senftle TP, Hong S, Islam MM, et al. The ReaxFF reactive force-field: development, applications and future directions. *NPJ Comput Mater.* **2016** Apr 3;2:15011.
- [102] Xu Y, Musgrave CB. A DFT study of the Al_2O_3 atomic layer deposition on SAMs: effect of SAM termination. *Chem Mater.* **2004** Feb 1;16:646–653.
- [103] Ali AA, Hashim AM. Density functional theory study of atomic layer deposition of Zinc Oxide on Graphene. *Nanoscale Res Lett.* **2015** July 22;10:299.
- [104] Elliott SD, Dey G, Maimaiti Y. Classification of processes for the atomic layer deposition of metals based on mechanistic information from density functional theory calculations. *J Chem Phys.* **2017**;146:052822.
- [105] Russo MF, van Duin ACT. Atomistic-scale simulations of chemical reactions: bridging from quantum chemistry to engineering. *Nucl Instrum Methods Phys Res A.* **2011** July 15;269:1549–1554.
- [106] Kim Y, Lee J, Yeom MS, et al. Strengthening effect of single-atomic-layer graphene in metal-graphene nanolayered composites. *Nat Commun.* **2013** July 2;4:2114.
- [107] Kim EJ, Chagarov E, Cagnon J, et al. Atomically abrupt and unpinned $\text{Al}_2\text{O}_3/\text{In}0.53\text{Ga}0.47\text{As}$ interfaces: experiment and simulation. *J Appl Phys.* **2009**;106:124508.
- [108] Hu X, Schuster J, Schulz SE, et al. Surface chemistry of copper metal and copper oxide atomic layer deposition from copper(ii) acetylacetone: a combined first-principles and reactive molecular dynamics study. *Phys Chem Chem Phys.* **2015**;17:26892–26902.
- [109] Heiranian M, Farimani AB, Aluru NR. Water desalination with a single-layer MoS(2) nanopore. *Nat Commun.* **2015**;6:8616.
- [110] Hu Z, Shi J, Heath Turner C. Molecular dynamics simulation of the Al_2O_3 film structure during atomic layer deposition. *Mol Simulat.* **2009** Apr 1;35:270–279.
- [111] Weckman T, Laasonen K. First principles study of the atomic layer deposition of alumina by TMA-H₂O-process. *Phys Chem Chem Phys.* **2015**;17:17322–17334.
- [112] Rapaport DC, Blumberg RL, McKay SR, et al. The art of molecular dynamics simulation. *Comput Phys.* **1996**;10:456.
- [113] Schneider J, Hamaekers J, Chill ST. ATK-ForceField: a new generation molecular dynamics software package. *Modelling Simul. Mater. Sci. Eng.* **2017**;25:085007 (28pp). IOP Publishing.
- [114] A. T. (ATK). QuantumWise simulator A/S [Online]. [cited 2018 Sep 15]. Available from: www.quantumwise.com
- [115] Pan D, Numerical and Experimental Studies of Atomic Layer Deposition for Sustainability Improvement. PhD, Mechanical Engineering, University of Wisconsin-Milwaukee, **2016**.
- [116] Pan D, Ma L, Xie Y, et al. Experimental and numerical investigations into the transient multi-wafer batch atomic layer deposition process with vertical and horizontal wafer arrangements. *Int J Heat Mass Transfer.* **2015** Dec 1;91:416–427.
- [117] Coetzee RA, Jen TC, Bhamjee M, et al. The mechanistic effect over the substrate in a square type atomic layer deposition reactor. presented at the International Journal of Modern Physics B, Chengdu, China, **2018**.
- [118] Coetzee RA, Jen TC, Bhamjee M, et al. The mechanistic effect over the substrate in a square type atomic layer deposition reactor. Presented at the International Conference of Material Science and Nanotechnology, Chengdu, China, **2018**.
- [119] Peltonen P, Vuorinen V, Marin G, et al. Numerical study on the fluid dynamical aspects of atomic layer deposition process. *J Vac Sci Technol A.* **2018**;36(2):021516.
- [120] Holmqvist A, Törndahl T, Stenström S. A model-based methodology for the analysis and design of atomic layer deposition processes—part II. *Chem Eng Sci.* **2013** May 3;94:316–329.
- [121] Holmqvist A, Törndahl T, Stenström S. A model-based methodology for the analysis and design of atomic layer deposition processes—part I: mechanistic modelling of continuous flow reactors. *Chem Eng Sci.* **2012** Oct 22;81:260–272.
- [122] Meyyappan M. Computational modeling in semiconductor processing. Norwood (MA): Artech House, Inc.; **1994**.
- [123] Gordon RG, Hausmann D, Kim E, et al. A kinetic model for step coverage by atomic layer deposition in narrow holes or trenches. *Chem Vap Deposition.* **2003**;9(2):73–78.
- [124] Shaeri MR, Jen T-C, Yuan CY. Reactor scale simulation of an atomic layer deposition process. *Chem Eng Res Des.* **2015** Feb 1;94:584–593.
- [125] Sungin Suh SP, Lim H, Choi YJ, et al. Investigation on spatially separated atomic layer deposition by gas flow simulation and depositing Al_2O_3 films. *J Vac Sci Technol A.* **2012**;30:051504.
- [126] Lu J, Elam JW, Stair PC. Atomic layer deposition—sequential self-limiting surface reactions for advanced catalyst “bottom-up” synthesis. *Surf Sci Rep.* **2016**;71:410–472.
- [127] Pan D, Guan D, Jen TC, et al. Atomic Layer Deposition Process Modeling and Experimental Investigation for Sustainable Manufacturing of Nano Thin Films, unpublished.
- [128] Deng Z, He W, Duan C, et al. Atomic layer deposition process optimization by computational fluid dynamics. *Vacuum.* **2016** Jan 1;123:103–110.
- [129] Gakis GP, Vergnes H, Scheid E, et al. Computational fluid dynamics simulation of the ALD of alumina from TMA and H₂O in a commercial reactor. *Chem Eng Res Des.* **2018** Apr 1;132:795–811.
- [130] Coetzee RAM, Jen TC, Lu J. The fluid flow effect on the inlet injection of the thin film deposition in a square type atomic layer deposition reactor. Presented at the International Conference on Sustainable Materials Processing and Manufacturing, South Africa, **2019**.
- [131] Olotu OO, Coetzee RAM, Olubambi PA, et al. The investigation of the exposure time effects with pressure in the atomic layer deposition process over micro-trench surface. Presented at the International Conference on Power and Energy Applications, Singapore, **2019**.
- [132] Li L, Xu W, Wu X, et al. Fabrication and characterization of infrared-insulating cotton fabrics by ALD. *Cellulose.* **2017** Sept 1;24:3981–3990.
- [133] Lee W, Jeon W, An CH, et al. Improved initial growth behavior of SrO and SrTiO₃ films grown by atomic

- layer deposition using $\{\text{Sr}(\text{demamp})(\text{tmhd})\}_2$ as Sr-precursor. *Chem Mater.* **2015** June 9;27:3881–3891.
- [134] Cleveland ER, Banerjee P, Perez I, et al. Profile evolution for conformal atomic layer deposition over nanotopography. *ACS Nano.* **2010** Aug 24;4:4637–4644.
- [135] Klesko JP, Rahman R, Dangerfield A, et al. Selective atomic layer deposition mechanism for titanium dioxide films with $(\text{EtCp})\text{Ti}(\text{NMe}_2)_3$: ozone versus water. *Chem Mater.* **2018**;30:970–981.
- [136] Sijung Y, Chanyoung Y, Eui-Sang P, et al. Chemical interactions in the atomic layer deposition of Ge-Sb-Se-Te films and their ovonic threshold switching behavior. *J Mater Chem C.* **2018**;6:5025–5032.
- [137] Hoffmann L, Brinkmann KO, Malerczyk J, et al. Spatial atmospheric pressure atomic layer deposition of Tin Oxide as an impermeable electron extraction layer for Perovskite solar cells with enhanced thermal stability. *ACS Appl Mater Interfaces.* **2018**;10:6006–6013.
- [138] Mattinen M, King PJ, Khriachtchev L, et al. Low-temperature wafer-scale deposition of continuous 2D SnS_2 films. *Small.* **2018**;14:1800547.
- [139] Lee J-H, Kim J-H, Sub Kim S. CuO-TiO₂p-n core-shell nanowires: sensing mechanism and p/n sensing-type transition. *Appl Surf Sci.* **2018**;448:489–497.
- [140] Fu Y, Jiang Y-B, Dunphy D, et al. Ultra-thin enzymatic liquid membrane for CO_2 separation and capture. *Nat Commun.* **2018**;9:1–12.
- [141] Yang W, Ahn J, Oh Y, et al. Adjusting the anisotropy of 1D Sb_2Se_3 nanostructures for highly efficient photoelectrochemical water splitting. *Adv Energy Mater.* **2018**;8:1702888.
- [142] Lemaire PC, Lee DT, Zhao J, et al. Reversible low-temperature metal node distortion during atomic layer deposition of Al_2O_3 and TiO_2 on $\text{UiO}-66-\text{NH}_2$ metal–organic framework crystal surfaces. *ACS Appl Mater Interfaces.* **2017**;9:22042–22054.
- [143] Park T, Kim H, Leem M, et al. Atomic layer deposition of Al_2O_3 on MoS_2 , WS_2 , WSe_2 , and h-BN: surface coverage and adsorption energy. *RSC Adv.* **2017**;7:884–889.
- [144] Austin DZ, Jenkins MA, Allman D, et al. Atomic layer deposition of ruthenium and ruthenium oxide using a zero-oxidation state precursor. *Chem Mater.* **2017**;29:1107–1115.
- [145] Jurca T, Moody MJ, Henning A, et al. Low-temperature atomic layer deposition of MoS_2 films. *Angew Chem.* **2017**;56:4991–4995.
- [146] Riha SC, Koegel AA, Emery JD, et al. Low-temperature atomic layer deposition of CuSbS_2 for thin-film photovoltaics. *ACS Appl Mater Interfaces.* **2017**;9:4667–4673.
- [147] Yang L, Jiang L, Fu W, et al. TiO_2 quantum dots grown on graphene by atomic layer deposition as advanced photocatalytic hybrid materials. *Appl Phys A Mater Sci Process.* **2017**;123:1–6.
- [148] Saric I, Peter R, Piltaver IK, et al. Residual chlorine in TiO_2 films grown at low temperatures by plasma enhanced atomic layer deposition. *Thin Solid Films.* **2017**;628:142–147.
- [149] Song GY, Oh C, Sinha S, et al. Facile phase control of multivalent vanadium oxide thin films (V_2O_5 and VO_2) by atomic layer deposition and postdeposition annealing. *ACS Appl Mater Interfaces.* **2017**;9:23909–23917.
- [150] Mäkelä M, Hatanpää T, Mizohata K, et al. Studies on thermal atomic layer deposition of silver thin films. *Chem Mater.* **2017**;29:2040–2045.
- [151] Qiao Q, Li YW, Zhang JZ, et al. Experimental investigations of the bismuth oxide film grown by atomic layer deposition using triphenyl bismuth. *Thin Solid Films.* **2017**;622:65–70.
- [152] Kim WJ, Jang E, Park TJ. Enhanced visible-light photocatalytic activity of $\text{ZnS}/\text{g-C}_3\text{N}_4$ type-II heterojunction nanocomposites synthesized with atomic layer deposition. *Appl Surf Sci.* **2017**;419:159–164.
- [153] Song SJ, Park T, Yoon KJ, et al. Comparison of the atomic layer deposition of tantalum oxide thin films using $\text{Ta}(\text{NtBu})(\text{NEt}_2)_3$, $\text{Ta}(\text{NtBu})(\text{NEt}_2)_2\text{Cp}$, and H_2O . *ACS Appl Mater Interfaces.* **2017**;9:537–547.
- [154] Kerrigan MM, Klesko JP, Winter CH. Low temperature, selective atomic layer deposition of cobalt metal films using Bis(1,4-di-tert-butyl-1,3-diazadienyl) cobalt and alkylamine precursors. *Chem Mater.* **2017**;29:7458–7466.
- [155] Zhang Y, Lu H-L, Wang T, et al. Photoluminescence enhancement of ZnO nanowire arrays by atomic layer deposition of ZrO_2 layers and thermal annealing. *Phys Chem Chem Phys.* **2016**;18:16377–16385.
- [156] Liu C, Lü H, Yang T, et al. Ultrathin ZnO interfacial passivation layer for atomic layer deposited ZrO_2 dielectric on the p-In_{0.2}Ga_{0.8}As substrate. *Appl Surf Sci.* **2018** June 30;444:474–479.
- [157] Lu H-L, Xu M, Ding S-J, et al. Quantum chemical study of the initial surface reactions of HfO_2 atomic layer deposition on the hydroxylated GaAs(001)-4×2 surface. *Appl Phys Lett.* **2006**;89:162905.
- [158] Ye L, Gougousi T. In situ infrared spectroscopy study of the interface self-cleaning during the atomic layer deposition of HfO_2 on GaAs(100) surfaces. *Appl Phys Lett.* **2014**;105:121604.
- [159] Dong H, Brennan B, Zhernokletov D, et al. In situ study of HfO_2 atomic layer deposition on InP(100). *Appl Phys Lett.* **2013**;102:171602.
- [160] An J-K, Chung N-K, Kim J-T, et al. Effect of growth temperature on the structural and electrical properties of ZrO_2 films fabricated by atomic layer deposition using a $\text{CpZr}[\text{N}(\text{CH}_3)_2]_3/\text{C}_7\text{H}_8$ cocktail precursor. *Materials.* **2018**;11:386.
- [161] Mameli A, Verheijen MA, Karasulu B, et al. New process concepts towards area-selective atomic layer deposition and atomic layer etching of Zinc Oxide. In: Meeting abstracts. The Electrochemical Society; **2018**. p. 985.
- [162] Mameli A, Karasulu B, Verheijen MA, et al. Area-selective atomic layer deposition of ZnO by area activation using electron beam-induced deposition. *Chem Mater.* **2019** Jan 31.
- [163] Kim S, Lee S, Ham S-Y, et al. A kinetic study of ZnO atomic layer deposition: effects of surface hydroxyl concentration and steric hindrance. *Appl Surf Sci.* **2019** Mar 1;469:804–810.
- [164] Khan MF, Nazir G, Lermolenko VM, et al. Electrical and photo-electrical properties of MoS_2 nanosheets with and without an Al_2O_3 capping layer under various environmental conditions. *Sci Technol Adv Mater.* **2016** Dec 1;17:166–176.
- [165] Salameh S, Gómez-Hernández J, Goulas A, et al. Advances in scalable gas-phase manufacturing and processing of nanostructured solids: A review. *Particulology.* **2017** Feb 1;30:15–39.

- [166] Huo J, Yuan C. Nano-particle emissions from atomic layer deposition. 2012 IEEE International Symposium on Sustainable Systems and Technology (ISSST). Boston, MA: IEEE; 2012, pp. 1.
- [167] Ma L, Pan D, Xie Y, et al. Atomic layer deposition of Al_2O_3 process emissions. RSC Adv. 2015;5:12824–12829.
- [168] Lukas M, Maximilian G, Teresa DLA, et al. Unearthing [3-(Dimethylamino)propyl]aluminium(III) complexes as novel atomic layer deposition (ALD) Precursors for Al_2O_3 : synthesis, characterization and ALD process development. Chem A Eur J. 2017;23:10768–10772.
- [169] Yuan CY, Yangping S. Sustainable scale-up studies of Atomic Layer Deposition for microelectronics manufacturing. Proceedings of the 2010 IEEE International Symposium on Sustainable Systems and Technology; Arlington, VA; 2010, pp. 1–6.
- [170] Ma L, Pan D, Xie Y, et al. Experimental STUDY of process emissions from atomic layer deposition of Al_2O_3 under various temperatures and purge time. J Manuf Sci Eng. 2017;139:051013–051013-7.
- [171] Louwen A, Van Sark WGJHM, Schropp REI, et al. Life-cycle greenhouse gas emissions and energy pay-back time of current and prospective silicon heterojunction solar cell designs. Prog Photovoltaics Res Appl. 2015;23(10):1406–1428.
- [172] Derbyshire K. Managing ALD effluent. 2018 Jun 15. Available from: <http://semiengineering.com/managing-ald-effluent/>
- [173] Kim JB, Fuentes-Hernandez C, Potsavage Jr WJ, et al. Low-voltage InGaZnO thin-film transistors with Al_2O_3 gate insulator grown by atomic layer deposition. Appl Phys Lett. 2009;94:142107.
- [174] Ma AM, Gupta M, Afshar A, et al. Schottky barrier source-gated ZnO thin film transistors by low temperature atomic layer deposition. Appl Phys Lett. 2013;103:253503.
- [175] Tsukazaki A, Ohtomo A, Chiba D, et al. Low-temperature field-effect and magnetotransport properties in a ZnO based heterostructure with atomic-layer-deposited gate dielectric. Appl Phys Lett. 2008;93:241905.
- [176] Byeong-Yun O, Young-Hwan K, Hee-Jun L, et al. High-performance ZnO thin-film transistor fabricated by atomic layer deposition. Semicond Sci Technol. 2011;26:085007.
- [177] Lin -Y-Y, Hsu -C-C, Tseng M-H, et al. Stable and high-performance flexible ZnO thin-film transistors by atomic layer deposition. ACS Appl Mater Interfaces. 2015 Nov 14;7:22610–22617.
- [178] Levy DH, Freeman D, Nelson SF, et al. Stable ZnO thin film transistors by fast open air atomic layer deposition. Appl Phys Lett. 2008;92:192101.
- [179] Wrench JS, Brunell IF, Chalker PR, et al. Compositional tuning of atomic layer deposited MgZnO for thin film transistors. Appl Phys Lett. 2014;105:202109.
- [180] Liu R, Peng M, Zhang H, et al. Atomic layer deposition of ZnO on graphene for thin film transistor. Mater Sci Semicond Process. 2016 Dec 01;56:324–328.
- [181] Kim SH, Baek I-H, Kim DH, et al. Fabrication of high-performance p-type thin film transistors using atomic-layer-deposited SnO films. J Mater Chem C. 2017;5:3139–3145.
- [182] Ahn CH, Kim SH, Cho SW, et al. Double-layer channel structure based ZnO thin-film transistor grown by atomic layer deposition. Phys Status Solidi (RRL) Rapid Res Lett. 2014;8:328–331.
- [183] Oruc FB, Aygun LE, Donmez I, et al. Low temperature atomic layer deposited ZnO photo thin film transistors. J Vac Sci Technol A. 2015;33:01A105.
- [184] Yang J, Park JK, Kim S, et al. Atomic-layer-deposited ZnO thin-film transistors with various gate dielectrics. Phys Status Solidi A. 2012;209:2087–2090.
- [185] Hwang CS, Park SHK, Oh H, et al. Vertical channel ZnO thin-film transistors using an atomic layer deposition method. IEEE Electron Device Lett. 2014;35:360–362.
- [186] Li H, Han D, Liu L, et al. Bi-layer channel AZO/ZnO thin film transistors fabricated by atomic layer deposition technique. Nanoscale Res Lett. 2017 March 24;12:223.
- [187] Yoon S-M, Seong N-J, Choi K, et al. Effects of deposition temperature on the device characteristics of oxide thin-film transistors using In-Ga-Zn-O active channels prepared by atomic-layer deposition. ACS Appl Mater Interfaces. 2017 July 12;9:22676–22684.
- [188] Ahn CH, Senthil K, Cho HK, et al. Artificial semiconductor/insulator superlattice channel structure for high-performance oxide thin-film transistors. Sci Rep. 2013 Sep 24;3:2737.
- [189] El-Atab N, Alqatari S, Oruc FB, et al. Diode behavior in ultra-thin low temperature ALD grown zinc-oxide on silicon. AIP Adv. 2013;3:102119.
- [190] Chung YJ, Choi WJ, Kang SG, et al. A study on the influence of local doping in atomic layer deposited Al: ZnO thin film transistors. J Mater Chem C. 2014;2:9274–9282.
- [191] Huang R, Sun K, Kiang KS, et al. Forming-free resistive switching of tunable ZnO films grown by atomic layer deposition. Microelectron Eng. 2016;161:7–12.
- [192] Ma Q, Zheng H-M, Shao Y, et al. Atomic-layer-deposition of indium oxide nano-films for thin-film transistors. Nanoscale Res Lett. 2018 Jan 09;13:4.
- [193] Ding X, Li S, Song J, et al. Enhancement of electrical stability in IGZO thin-film transistors inserted with an izo layer grown by atomic layer deposition. J Nanoelectron Optoelectron. 2017;12:273–277.
- [194] Clark R. Emerging Applications for High K Materials in VLSI Technology. Materials. 2014;7:2913.
- [195] Assaud L, Hanbücken M, Santinacci L. Atomic layer deposition of TiN/ Al_2O_3 /TiN nanolaminates for capacitor applications. ECS Trans. 2013 March 15;50:151–157.
- [196] Groenland AW, Wolters RAM, Kovalgin AY, et al. A difference in using atomic layer deposition or physical vapour deposition TiN as electrode material in metal-insulator-metal and metal-insulator-silicon capacitors. J Nanosci Nanotechnol. 2011;11:8368–8373.
- [197] Austin DZ, Allman D, Price D, et al. Plasma enhanced atomic layer deposition of $\text{Al}_2\text{O}_3/\text{SiO}_2$ MIM capacitors. IEEE Electron Device Lett. 2015;36:496–498.
- [198] Austin DZ, Atomic layer deposition of multi-insulator metal-insulator-metal capacitors. Doctor of Philosophy (Ph.D.), Electrical and Computer Engineering, Oregon State University, Oregon State University, 2017.
- [199] Park B-E, Oh I-K, Mahata C, et al. Atomic layer deposition of Y-stabilized ZrO₂ for advanced DRAM capacitors. J Alloys Compd. 2017 Oct 25;722:307–312.
- [200] Xie D, Feng T, Luo Y, et al. Atomic layer deposition HfO₂ film used as buffer layer of the Pt/(Bi0.95Nd0.05)(Fe0.95Mn0.05)O₃/HfO₂/Si capacitors for feft application. J Adv Dielectr. 2011;01:369–377.

- [201] Peng K, Wang B, Xiao D, et al. TDDB improvement by optimized processes on metal-insulator-silicon capacitors with atomic layer deposition of Al_2O_3 and multi layers of TiN film structure. *J Semicond.* **2009**;30:082005.
- [202] Daubert JS, Wang R, Ovental JS, et al. Intrinsic limitations of atomic layer deposition for pseudocapacitive metal oxides in porous electrochemical capacitor electrodes. *J Mater Chem A*. **2017**;5:13086–13097.
- [203] Lee SW, Han JH, Han S, et al. Atomic layer deposition of SrTiO_3 thin films with highly enhanced growth rate for ultrahigh density capacitors. *Chem Mater.* **2011**;23:2227–2236.
- [204] Gaboriau D, Boniface M, Valero A, et al. Atomic layer deposition alumina-passivated silicon nanowires: probing the transition from electrochemical double-layer capacitor to electrolytic capacitor. *ACS Appl Mater Interfaces.* **2017**;9:13761–13769.
- [205] Iglesias L, Vega V, García J, et al. Development of electrostatic supercapacitors by atomic layer deposition on nanoporous anodic aluminum oxides for energy harvesting applications. *Front Phys.* **2015**;3:12.
- [206] Kim J-H, Kil D-S, Yeom S-J, et al. Modified atomic layer deposition of RuO_2 thin films for capacitor electrodes. *Appl Phys Lett.* **2007**;91:052908.
- [207] Guo T, Zhang G, Su X, et al. Transparent and flexible capacitors with an ultrathin structure by using graphene as bottom electrodes. *Nanomaterials.* **2017**;7:418.
- [208] Samsung, Exploring the Key Samsung Technologies That Enabled 10nm-Class DRAM, **2016**.
- [209] Liu C, Wang C-C, Kei C-C, et al. Atomic layer deposition of platinum nanoparticles on carbon nanotubes for application in proton-exchange membrane fuel cells. *Small.* **2009**;5:1535–1538.
- [210] Moghaddam S, Pengwang E, Jiang Y-B, et al. An inorganic–organic proton exchange membrane for fuel cells with a controlled nanoscale pore structure. *Nat Nanotechnol.* **2010**;5:230.
- [211] Lu J, Liu B, Greeley JP, et al. Porous alumina protective coatings on palladium nanoparticles by self-poisoned atomic layer deposition. *Chem Mater.* **2012** June 12;24:2047–2055.
- [212] Jiang Y-B, Xomeritakis G, Chen Z, et al. Sub-10 nm thick microporous membranes made by plasma-defined atomic layer deposition of a bridged silsesquioxane Precursor. *J Am Chem Soc.* **2007** Dec 01;129:15446–15447.
- [213] Shannon MA, Bohn PW, Elimelech M, et al. Science and technology for water purification in the coming decades. *Nature.* **2008** March 20;452:301–310.
- [214] Tal A. Seeking Sustainability: Israel's evolving water management strategy. *Science.* **2006**;313:1081–1084.
- [215] Service RF. Desalination freshens up. *Science.* **2006**;313:1088–1090.
- [216] Xu GR, Xu JM, Feng HJ, et al. Tailoring structures and performance of polyamide thin film composite (PA-TFC) desalination membranes via sublayers adjustment—a review. *Desalination.* **2017**;417:19–35.
- [217] Geise GM, Lee H-S, Miller DJ, et al. Water purification by membranes: the role of polymer science. *J Polym Sci B Polym Phys.* **2010**;48:1685–1718.
- [218] Lee KP, Arnot TC, Mattia D. A review of reverse osmosis membrane materials for desalination—development to date and future potential. *J Membr Sci.* **2011** March 15;370:1–22.
- [219] Salta M, Wharton JA, Stoodley P, et al. Designing biomimetic antifouling surfaces. *Philos Trans R Soc A Math Phys Eng Sci.* **2010**;368(1929):4729–4754.
- [220] Jing Zhaoa XZ, Jianga Z, Lia Z, et al. Biomimetic and bioinspired membranes: preparationand application. Elsevier. **2014** September;33:1668–1720.
- [221] Lohi AAHDA. Applications of biomimetic and bioinspired membranes, biomimetic and bioinspired membranes for new frontiers in sustainable water treatment technology. Rijeka (Croatia): IntechOpen; **2017** December 6th.
- [222] Miikkulainen V, Leskelä M, Ritala M, et al. Crystallinity of inorganic films grown by atomic layer deposition: overview and general trends. *J Appl Phys.* **2013**;113:021301.
- [223] Rempe SC, Brinker J, Rogers DM, et al. Biomimetic membranes and methods of making biomimetic membranes. U.S. Patent 9,486,742, issued November 8, **2016**.
- [224] Brinker CJ, Lu Y, Sellinger A, et al. Evaporation-induced self-assembly: nanostructures made easy. *Adv Mater.* **1999**;11:579–585.
- [225] Kumar M, Grzelakowski M, Zilles J, et al. Highly permeable polymeric membranes based on the incorporation of the functional water channel protein Aquaporin Z. *Proc Nat Acad Sci.* **2007** Dec 26;104:20719–20724.
- [226] Pendergast MM, Hoek EMV. A review of water treatment membrane nanotechnologies. *Energy Environ Sci.* **2011**;4:1946–1971.
- [227] Giwa A, Hasan SW, Yousuf A, et al. Biomimetic membranes: A critical review of recent progress. *Desalination.* **2017** Oct 15;420:403–424.
- [228] Li Z, Valladares Linares R, Bucs S, et al. Aquaporin based biomimetic membrane in forward osmosis: chemical cleaning resistance and practical operation. *Desalination.* **2017**;420:208–215.
- [229] Ferrari AC, Basko DM. Raman spectroscopy as a versatile tool for studying the properties of graphene. *Nat Nanotechnol.* **2013** April 04;8:235.
- [230] Vervuurt RHJ, Kessels WMM, Bol AA. Atomic layer deposition for graphene device integration. *Adv Mater Interfaces.* **2017**;4:1700232.
- [231] Balandin AA. Thermal properties of graphene and nanostructured carbon materials. *Nat Mater.* **2011** July 22;10:569.
- [232] Wang L, Travis JJ, Cavanagh AS, et al. Ultrathin oxide films by atomic layer deposition on Graphene. *Nano Lett.* **2012** July 11;12:3706–3710.
- [233] Alles H, Aarik A, Kozlova J, et al., Atomic layer deposition of High-k oxides on Graphene. *Graphene.* IntechOpen, **2011**. arXiv preprint arXiv:1109.4026.
- [234] Cohen-Tanugi D, Lin L-C, Grossman JC. Multilayer nanoporous graphene membranes for water desalination. *Nano Lett.* **2016** Feb 10;16:1027–1033.
- [235] Cohen-Tanugi D, Grossman JC. Water desalination across nanoporous Graphene. *Nano Lett.* **2012** July 11;12:3602–3608.

- [236] Seon LC, Moon-Ki C, Young HY, et al. Facilitated water transport through Graphene oxide membranes functionalized with aquaporin-mimicking peptides. *Adv Mater.* **2018**;30:1705944.
- [237] O'Neill BJ, Jackson DHK, Lee J, et al. Catalyst design with atomic layer deposition. *ACS Catal.* **2015**;5:1804–1825.
- [238] Cao K, Cai J, Liu X, et al. Review article: catalysts design and synthesis via selective atomic layer deposition. *J Vac Sci Technol A.* **2018**;36:010801.
- [239] Putkonen LSM, Koskinen-Soivi M-L, Kihlman J, et al. ALD for catalysis – new approaches for support materials, catalysts and overcoatings. Finland: VTT Technical Research Centre of Finland; **2015**.
- [240] Camacho-Bunquin J, Shou H, Aich P, et al. Catalyst synthesis and evaluation using an integrated atomic layer deposition synthesis-catalysis testing tool. *Rev Sci Instrum.* **2015**;86:084103.
- [241] Yeo JC, Lim CT. Emerging flexible and wearable physical sensing platforms for healthcare and biomedical applications. *Microsys Nanoeng.* **2016** Sep 26;2:16043.
- [242] Pang C, Lee C, Suh K-Y. Recent advances in flexible sensors for wearable and implantable devices. *J Appl Polym Sci.* **2013**;130:1429–1441.
- [243] Sokolov AN, Tee BCK, Bettinger CJ, et al. Chemical and engineering approaches to enable organic field-effect transistors for electronic skin applications. *Acc Chem Res.* **2012** March 03;45:361–371.
- [244] Im H, Wittenberg NJ, Lindquist NC, et al. Atomic layer deposition: A versatile technique for plasmonics and nanobiotechnology. *J Mater Res.* **2012**;27:663–671.
- [245] Narayan RJ, Monteiro-Riviere NA, Brigmon RL, et al. Atomic layer deposition of TiO₂ thin films on nanoporous alumina templates: medical applications. *JOM.* **2009** June 01;61:12–16.
- [246] Bilo F, Borgese L, Prost J, et al. Atomic layer deposition to prevent metal transfer from implants: an X-ray fluorescence study. *Appl Surf Sci.* **2015** Dec 30;359:215–220.
- [247] Juppo AM. Nanocoating of drug powders and minitablets with atomic layer deposition. Presented at the International Conference and Exhibition on Pharmaceutics & Novel Drug Delivery Systems, Berlin, Germany, **2018**.
- [248] Kääriäinen TO, Kemell M, Vehkämäki M, et al. Surface modification of acetaminophen particles by atomic layer deposition. *Int J Pharm.* **2017**;525:160–174.